Published in final edited form as:

Immunity. 2020 November 17; 53(5): 1063–1077.e7. doi:10.1016/j.immuni.2020.10.001.

Substance P release by sensory neurons triggers dendritic cell migration and initiates the Type-2 immune response to allergens

Caroline Perner[1,#], **Cameron H. Flayer**[1,#], **Xueping Zhu**[1,#], **Pamela A. Aderhold**[1,†], **Zaynah N. A. Dewan**[1,†], **Tiphaine Voisin**[2], **Ryan B. Camire**[1,2], **Ohn A. Chow**[1], **Isaac M. Chiu**[2], **Caroline L. Sokol**[1]

[1]Center for Immunology & Inflammatory Diseases, Division of Rheumatology, Allergy & Immunology, Massachusetts General Hospital, Harvard Medical School, Boston, MA 02114, USA

[2]Department of Immunology, Harvard Medical School, Boston, MA 02115, USA

SUMMARY

Dendritic cells (DCs) of the cDC2 lineage initiate allergic immunity and in the dermis are marked by their expression of CD301b. CD301b$^+$ dermal DCs respond to allergens encountered in vivo, but not in vitro. This suggests that another cell in the dermis may sense allergens and relay that information to activate and induce the migration of CD301b$^+$ DCs to the draining lymph node (dLN). Using a model of cutaneous allergen exposure, we show that allergens directly activated TRPV1$^+$ sensory neurons leading to itch and pain behaviors. Allergen-activated sensory neurons released the neuropeptide Substance P, which stimulated proximally located CD301b$^+$ DCs through the Mas-related G-protein coupled receptor member A1 (MRGPRA1). Substance P induced CD301b$^+$ DC migration to the dLN where they initiated T helper-2 cell differentiation. Thus, sensory neurons act as primary sensors of allergens, linking exposure to activation of allergic-skewing DCs and the initiation of an allergic immune response.

Graphical Abstract

Further information and requests for resources and reagents should be directed to and will be fulfilled by the Lead Contact, Caroline Sokol (CLSOKOL@mgh.harvard.edu).

[#]These authors contributed equally to this work.

[†]These authors contributed equally to this work.

AUTHOR CONTRIBUTIONS

C.P., C.H.F., X.Z., P.A.A., Z.N.A.D., and C.L.S. designed the study. C.P., C.H.F., X.Z., P.A.A., Z.N.A.D., T.V., R.B.C., O.A.C., and C.L.S. performed and/or analyzed experiments. C.P., C.H.F., P.A.A., Z.N.A.D., and C.L.S. wrote the manuscript. I.M.C. provided resources and advice. C.L.S. provided resources, reagents and funding. C.L.S. supervised the study.

DECLARATION OF INTERESTS

C.L.S. is a paid consultant for Bayer and Merck. P.A.A. is a current employee of Skyhawk Therapeutics. I.M.C. receives sponsored research support from GSK and Allergan Pharmaceuticals. I.M.C. is on the scientific advisory boards of GSK and Kintai Pharmaceuticals.

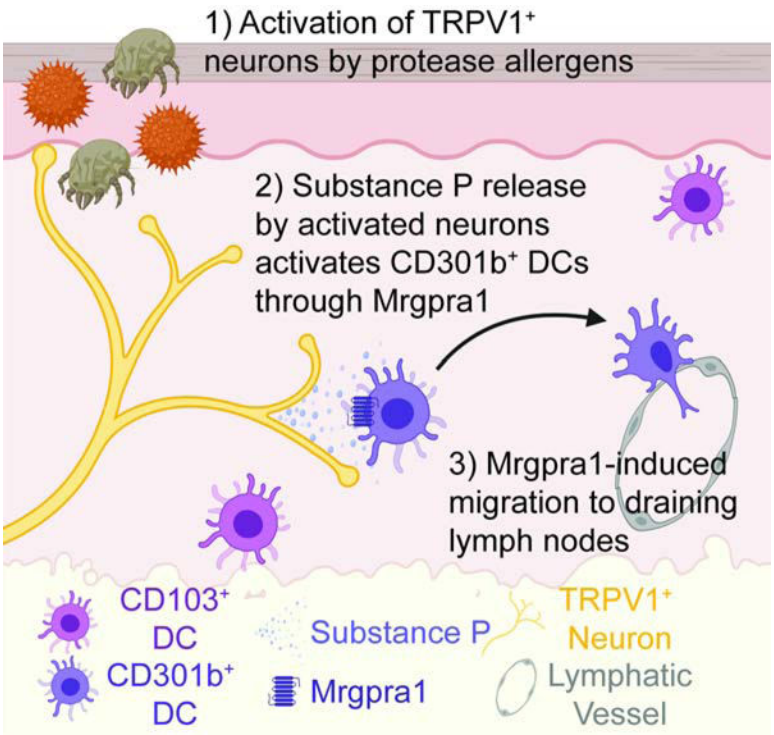

eTOC BLURB

Dendritic cells are required for the initiation of the allergic immune response, but it is unclear how they sense allergens. Perner et al reveal that allergen induced Substance P release by TRPV1+ sensory neurons triggers MRGPRA1-dependent dendritic cell migration to the lymph node where they initiate the allergic immune response.

Keywords

Dendritic cells; sensory neurons; TRPV1; Substance P; Th2; allergy; chemotaxis; MRGPRA1

INTRODUCTION

Allergic diseases are characterized by inappropriate Type-2 immune responses targeted against non-infectious environmental antigens and venoms. Defective cutaneous barriers permit the entry of food and environmental allergens into the body where they can ultimately activate the immune system, but the precise mechanisms by which allergens are sensed by the innate immune system remain unclear (Strid et al., 2004). Dendritic cells (DCs) are innate immune cells that link pathogen sensing with adaptive immune activation. Immature DCs actively sample their environment for evidence of pathogens that are detected through their pattern recognition receptors (PRRs). Upon PRR ligation, DCs undergo a complex process of maturation that culminates in their migration to the draining lymph node (dLN), where they present antigen and provide costimulation to naïve T cells. Thus, DCs link innate immune sensing with adaptive immune activation.

Conventional DCs (cDC) can be divided into two main subsets based on transcription factor dependence and functional characteristics. cDC1s are dependent upon interferon regulatory factor 8 (IRF8) and are specialized in antigen cross-presentation, while cDC2s are dependent upon interferon regulatory factor 4 (IRF4) and are specialized in T helper cell differentiation. T helper-2 (Th2) cell-skewing cDC2s, are dependent upon both IRF4 and Kruppel like factor 4 (KLF4), and in the skin this population is characterized by its surface expression of CD301b. CD301b$^+$ DCs migrate to the dLN and are required for Th2 cell differentiation after cutaneous exposure to allergens and helminth parasites (Gao et al., 2013; Kumamoto et al., 2013; Tussiwand et al., 2015). In the Type-1 immune response to bacteria and viruses, DC maturation is marked by the upregulation of the chemokine receptor CCR7. This CCR7 upregulation acts in the fashion of a molecular switch, endowing the mature DC to sense and migrate towards gradients of the chemokine CCL21 that are homeostatically produced by the lymphatic endothelium (Ohl et al., 2004). Although cutaneous allergen exposure leads to CCR7-dependent CD301b$^+$ DC migration from the skin to the dLN, it does not lead to CCR7 upregulation (Sokol et al., 2018). In the absence of this molecular switch, what is the primary signal that initiates CD301b$^+$ DC migration out of the skin in response to allergens? Similarly, although CD301b$^+$ DCs are activated by allergens in vivo and required for Th2 cell differentiation, CD301b$^+$ DCs exposed to allergens in vitro are incapable of promoting Th2 cell differentiation in vitro or after in vivo transfer (Kumamoto et al., 2013). How do CD301b$^+$ DCs sense allergens in vivo?

Type-2 immunogens are a varied group of simple protein allergens, secreted molecules from helminth parasites, and venoms (Palm et al., 2012). Many immunodominant Type-2 immunogens share in common intrinsic or induced enzymatic activity that is required for their immunogenicity, but how they activate the innate immune system is unclear (Lamhamedi-Cherradi et al., 2008; Palm et al., 2013; Porter et al., 2009; Sokol et al., 2008; Van Dyken and Locksley, 2018). Instead of direct detection, DCs may detect endogenous alarmins that are released in response to allergen exposure. Enzymatically active allergens such as cysteine proteases induce the release and activation of innate alarmins such as interleukin-33 (IL-33) and thymic stromal lymphopoietin (TSLP) (Cayrol et al., 2018; Tang et al., 2010). Indeed, DCs express the IL-33 receptor ST2 and IL-33 stimulation of DCs can promote Th2 cell skewing (Rank et al., 2009). IL-33 can also stimulate innate lymphoid cells, which can indirectly enhance DC migration to dLNs (Halim et al., 2014). Likewise, TSLP is produced by epithelia in the setting of chronic allergic inflammation and promotes DC activation (Liu et al., 2007). However, data from alarmin-deficient models show only a partial role for alarmins in allergen-induced DC migration and activation (Besnard et al., 2011; Halim et al., 2014). This led us to hypothesize the existence of a primary cellular sensor of allergens that not only senses the presence of allergens, but also relays critical cues to initiate the migration of allergic, or Th2 cell-skewing, CD301b$^+$ DCs to the dLN.

One potential allergen sensor is the sensory nervous system, which is highly concentrated in barrier epithelia, broadly responsive to many different stimuli, and directly activated in vitro by diverse enzymatically active allergens such as bee venom, house dust mites (HDM), and papain (Chen and Lariviere, 2010; Reddy and Lerner, 2010; Serhan et al., 2019; Talbot et al., 2016; Trier et al., 2019; Veiga-Fernandes and Mucida, 2016). Sensory neurons have been shown to be closely associated with Langerhans cells in the human epidermis and activation

of corneal sensory neurons can lead to DC activation in the contralateral eye (Guzman et al., 2018; Hosoi et al., 1993). Based on this, we hypothesized a two-step model for allergen activation of DCs wherein allergens activate sensory neurons leading to their local release of neuropeptides (Step 1), which then act upon local DCs to promote their migration (Step 2) to the dLN where they can activate naïve T cells to promote Th2 cell differentiation. Using the model cysteine protease allergen papain, we found that papain induced an immediate sensory response in naïve mice. Papain directly activated a subset of sensory neurons that are enriched in TRPV1$^+$ neurons to release Substance P (SP). SP then acted on proximally located Th2 cell-skewing dermal CD301b$^+$ DCs through their expression of a SP receptor *Mrgpra1* to promote their migration to the dLN. Depletion of TRPV1$^+$ neurons, inhibition of sensory neuronal activation, or ablation of *Mrgpra1* from CD301b$^+$ DCs led to a defect in CD301b$^+$ DC migration and as a direct consequence, Th2 cell differentiation. Thus, sensory neurons play an essential role in allergen recognition, DC activation, and initiation of the allergic immune response.

RESULTS

Allergens induce immediate and transient itch responses in naïve mice

To investigate the role of sensory neurons in allergen recognition in vivo, we utilized the model allergen papain that induces robust CD301b$^+$ DC migration, Th2 cell differentiation and IgE production with defined kinetics after one cutaneous exposure to the enzymatically active allergen (Kumamoto et al., 2013; Sokol et al., 2008). Intradermal (i.d.) papain injection of mice led to an immediate and transient mixed itch (scratching bouts) and pain (wiping bouts) response that was dependent on its protease activity (Fig. 1A–D). Papain-induced sensory responses were overall comparable to the established itch and pain triggers, histamine and capsaicin, respectively (Fig. 1A–D). The sensory response was not specific to papain as Alternaria extract also induced an itch response (Fig. 1A). To investigate what neurons were involved in the sensory response to allergens, we co-injected papain with the lidocaine derivative QX314 that blocks sodium channel activation of neurons after entering through large-pore cation channels including TRPV1 and TRPA1 (Binshtok et al., 2007; Roberson et al., 2013). Co-injection of papain and 1% QX314 blocked the allergen-induced sensory response (Fig. 1E and F), suggesting a role for TRPV1$^+$ neurons in direct allergen sensing.

Allergens directly activate a population of sensory neurons enriched in TRPV1$^+$ neurons

The cell bodies of cutaneous sensory neurons are contained in dorsal root ganglia (DRG) adjacent to the spinal cord. To test whether papain could directly activate sensory neurons, we performed calcium (Ca^{2+}) flux analysis of cultured DRG neurons in response to sequential exposure with different stimuli. Papain induced robust Ca^{2+} influx in DRG neurons within seconds of administration (Fig. 2A & B). Using potassium chloride (KCl) responsiveness as a marker of live neurons, we found that approximately 16% of neurons were responsive to papain (Fig. 2C), a similar value to that reported for HDM responsive neurons (Serhan et al., 2019). TRPV1 expression defines a subset of nociceptive neurons that not only sense noxious heat, but also promote pruriceptive responses. TRPV1$^+$ neurons are directly activated by HDM cysteine protease allergens and have been associated with

allergic inflammation (Roberson et al., 2013; Serhan et al., 2019; Talbot et al., 2015; Trankner et al., 2014). If the papain responsive neurons were enriched in TRPV1$^+$ neurons, we would expect to see a greater percentage of TRPV1$^+$ neurons in this group. Indeed, whereas capsaicin responsive neurons (TRPV1$^+$) made up about 35% of the total neurons, they represented an average of 68% of the papain responsive neurons (Fig. 2C–E). A minority of papain-responsive neurons were also activated by the itch inducing ligands histamine and/or chloroquine, suggesting that papain-responsive neurons are a heterogenous population of previously described NP2, NP3 and PEP1 sensory neuron subclasses (Fig. 2D and E) (Usoskin et al., 2015). Given that papain-responsive neurons strongly overlapped with TRPV1$^+$ (capsaicin-responsive) neurons, we next asked whether the papain-induced sensory response would be affected by depletion of noxious heat-sensing TRPV1$^+$ neurons. Diphtheria toxin (DT) injection into *Trpv1^{DTR}* mice, which express the human diphtheria toxin receptor (DTR) under control of the *Trpv1* promoter, specifically depletes TRPV1$^+$ neurons in the DRG and vagal ganglia (Baral et al., 2018; Pogorzala et al., 2013; Trankner et al., 2014). Consistent with depletion of TRPV1$^+$ neurons, DT treated *Trpv1^{DTR}* mice lost their tail flick response to noxious heat and *Trpv1* gene expression in the DRG (Fig. 2F and G). Deletion of *Trpv1$^+$* neurons led to a loss of the itch response and a partial block in the pain response to papain (Fig. 2H and I), indicating that papain activates TRPV1$^+$ neurons in vitro and in vivo.

Dendritic cells do not directly respond to the cysteine protease allergen papain

DCs directly detect bacterial and viral pathogen associated molecular patterns (PAMPs) through their direct binding to DC PRRs. This leads to DC maturation, marked by the upregulation of antigen presentation, costimulatory molecules, and CCR7. Thus, maturation promotes the migration of DCs with unique T cell activating capability to the dLN. Consistent with the direct activation of DCs by PAMPs, CD301b$^+$ DCs exposed to lipopolysaccharide (LPS) in vivo or in vitro upregulated the activation markers PDL2, CD86 and MHC Class II (Fig. 3A and B, Fig. S1A–D). Papain immunization induced PDL2 upregulation, but in vitro papain stimulation at concentrations up to 100 μg/ml had no effect on PDL2, CD86 or MHC Class II expression on CD301b$^+$ DCs (Fig. 3A and B, Fig. S1A–E). At higher concentrations, overnight papain stimulation led to a decrease in PDL2 and CD86 expression possibly due to proteolytic cleavage (Fig. S1E). Immunization with papain and LPS also led to an increase in the chemotactic activity of CD301b$^+$ DCs (Fig. 3C), while in vitro exposure with papain had no effect (Fig. 3D). These observations suggest that DCs do not independently detect allergens.

CD301b$^+$ dendritic cells colocalize with sensory neurons

Given our observations that sensory neurons, but not DCs, are directly activated by allergens, we hypothesized that allergens are detected by sensory neurons that then relay this signal to local DCs. To determine whether sensory neurons could be physically interacting with CD301b$^+$ DCs in vivo, we imaged the naïve skin of *Nav1.8$^{cre/+}$ tdTomato^{loxSTOPlox}* reporter mice (*Nav1.8^{tdTomato}*) where *Nav1.8*-lineage nociceptive sensory neurons are marked by tdTomato expression (Stirling et al., 2005). CD301b$^+$ DCs were localized in close proximity to the Nav1.8$^+$ nerve fibers in the naïve dermis (Fig. 3E). Furthermore, CD301b$^+$ DCs were significantly closer to sensory neurons than were their CD301b$^-$ counterparts,

which in the dermis include the Th1 cell-skewing cDC1 and the Th17 cell-skewing subset of cDC2 (Fig. 3F). Given these observations as well as the known interplay between sensory neurons and CD301b$^+$ DCs in Candida infection (Kashem et al., 2015), we hypothesized that the spatial relationship between sensory neurons and CD301b$^+$ DCs could reflect a functional requirement for neuronal stimulation specific to allergen-responsive CD301b$^+$ DCs in the dermis.

TRPV1$^+$ sensory neuron activation is required for allergen-induced CD301b$^+$ DC migration

We hypothesized that sensory neurons, activated by allergens, may relay a signal to closely associated CD301b$^+$ DCs to activate their allergen-induced migration to the dLN. To assess allergen-induced CD301b$^+$ DC migration, we used Kaede mice that express a photoconvertible green to red fluorescent protein, which allows the tracking of cells originating from the site of photoconversion and allergen exposure (Kaede^{red}) (Tomura et al., 2008). As previously described, papain immunization led to a specific migration of CD301b$^+$ DCs from the photoconverted skin to the dLN (Fig. 4A) (Sokol et al., 2018). QX314 co-injection blocked this papain-induced migration of skin emigrant, Kaede^{red}, CD301b$^+$ DCs to the dLN (Fig. 4A), suggesting a role for sensory neuron activation in CD301b$^+$ DC migration in vivo. To evaluate possible DC-specific effects of QX314 we performed in vitro chemotaxis assays of bone marrow derived DCs (BMDCs). Although higher concentrations inhibited migration, 1% QX314 had no effect on BMDC migration in vitro, indicating a specific role for neurons in allergen-induced DC migration (Fig. 4B).

Given our data that papain activated a population of neurons enriched in TRPV1$^+$ sensory neurons (Fig. 2D, 2E, 2H and I), we hypothesized that TRPV1$^+$ neurons would be required for papain-induced CD301b$^+$ DC migration. We generated Kaede x *Trpv1*^{DTR} mice and performed DT-mediated depletion of *Trpv1*$^+$ neurons. To evaluate the specificity of *Trpv1*^{DTR} mediated depletion, we first assessed *Trpv1* expression in a published murine skin scRNASeq dataset as well as in cutaneous immune cells from the Immunological Genome Consortium (Immgen) microarray dataset and found no *Trpv1* expression in these cells (Fig. S2A and B) (Heng et al., 2008; Joost et al., 2020). We next verified this by examining the frequency of cutaneous immune cells after DT-mediated depletion. Although mice depleted of TRPV1$^+$ cells showed a significant increase in total DCs and mast cells, there was no decrease in percentage of immune cell subsets in the skin, illustrating the specificity of *Trpv1*^{DTR} depletion for sensory neurons in the skin (Fig. S2C). Although there was no difference in dLN cellularity, papain-immunized Kaede x *Trpv1*^{DTR} mice showed a loss of Kaede^{red} CD301b$^+$ DCs in the dLN compared with Kaede mice (Fig. 4C and D). TRPV1$^+$ neuronal depletion had no effect on the frequency or number of CD301b$^+$ DCs in the naïve dermis (Fig. 4E), indicating that disrupted CD301b$^+$ DC migration to the dLN was due to a specific defect in papain-induced migration. Alternaria extract similarly led to CD301b$^+$ DC migration from the skin to the dLN that was blocked by QX314, indicating that sensory neuron activation may be a global requirement for allergen-induced CD301b$^+$ DC migration (Fig. 4F). This requirement for sensory neuron activation was specific to allergen-induced CD301b$^+$ DC migration. There was no effect of QX314 on the migration of CD103$^+$ DCs (including cDC1 and Th17 cell-skewing cDC2s in the dermis) after immunization with OVA and LPS (Fig. 4G).

Substance P release from sensory neurons induces CD301b$^+$ DC migration

Our data suggested that TRPV1$^+$ sensory neurons directly sense cysteine protease allergens and relay signals to promote the egress of local Th2 cell skewing CD301b$^+$ DCs to the dLN. Activated peptidergic TRPV1$^+$ neurons can release SP in response to allergen exposure and calcitonin gene-related peptide (CGRP) in response to bacterial and fungal exposures (Baral et al., 2018; Chiu et al., 2013; Cohen et al., 2019; Kashem et al., 2015; Pinho-Ribeiro et al., 2018; Serhan et al., 2019). Papain immunization promoted SP and inhibited CGRP release from skin explants (Fig. 5A). This pattern of neuropeptide release was also seen after direct stimulation of DRG cultures with both papain and HDM extract (Fig. 5B and S3), indicating that cysteine protease allergens directly stimulate neuropeptide release from sensory neurons. Consistent with this, SP release from skin explants was inhibited by co-injection with QX314 (Fig. 5C). In contrast to another report, we found that Alternaria extract, which has serine protease activity, was also capable of inducing DRG release of SP and inhibition of CGRP (Fig. S3) (Cayrol et al., 2018; Serhan et al., 2019). These data indicate that the capacity for sensory neuron activation and SP release may be shared amongst disparate allergens.

We next examined the role of SP in promoting CD301b$^+$ DC migration. The *Tac1* gene encodes for three neuropeptides: SP, Neurokinin A, and Neurokinin K. *Tac1* was not enriched in cutaneous immune cells (Fig. S2A and B) and despite its role as a pruritogen *Tac1*$^{-/-}$ mice exhibited intact itch responses to papain (Fig. S2D). However, *Tac1*$^{-/-}$ mice did show a decrease in the percent and total number of activated (PDL2$^+$) CD301b$^+$ DCs in the dLN 24 hours after papain immunization (Fig. 5D). To specifically assess the role of SP and CGRP in CD301b$^+$ DC migration from the skin, we injected photoconverted skin of Kaede mice with OVA and CGRP or SP. Although CGRP had no effect on CD301b$^+$ or CD103$^+$ DC migration, SP injection robustly induced the migration of Kaede^{red} CD301b$^+$ DCs to the dLN (Fig. 5E–G). This SP effect was specific to the migration of Th2 cell skewing CD301b$^+$ DCs; Th1 and Th17 cell-skewing CD103$^+$ dermal DCs were unaffected by SP injection (Fig 5F–G).

We next examined the role of sensory neurons in CD301b$^+$ DC migration using a patch application model of epicutaneous allergen administration (Fig. S4A) (Deckers et al., 2017; Iida et al., 2014). Papain induced robust CD301b$^+$ DC migration as well as a trend for increased SP release from skin explants 24 hours after patch placement (Fig. S4B–D). Application of a single patch led to modest Th2 cell differentiation that was dependent on CD301b$^+$ cells (Fig. S4E), underscoring the role for CD301b$^+$ DCs in both i.d. and epicutaneous allergen administration. Despite differences in sensory neuron innervation of epidermis and dermis (Usoskin et al., 2015; Zylka et al., 2005), we found that papain-induced CD301b$^+$ DC migration was significantly decreased in mice depleted of *Trpv1*$^+$ neurons (Fig. S4F and G). Thus, TRPV1$^+$ neurons act as global regulator of allergen-induced CD301b$^+$ DC migration.

Allergen-induced Substance P release and CD301b$^+$ DC migration is mast cell independent

Bidirectional interactions between mast cells and DCs promote both of their functions. Mast cells promote the migration of DCs to the dLN (Dawicki et al., 2010; Mazzoni et al., 2006;

Serhan et al., 2019; Shelburne et al., 2009). Conversely, DCs can transfer antigens to mast cells, thereby promoting their degranulation (Choi et al., 2018). To investigate whether mast cells were involved in our model, we injected papain i.d. in wild type or mast cell deficient *Kit*$^{W\text{-}sh/W\text{-}sh}$ mice. c-Kit is expressed by nociceptive neurons and signaling through c-Kit has been shown to prime some TRPV1-mediated responses in nociceptive neurons (Hirata et al., 1993; Milenkovic et al., 2007; Takagi et al., 2008). Thus, any loss of response in Kit mutant mice would be difficult to assign to their mast cell deficiency or sensory neuron defects. However, we found that the sensory response to papain was unaffected in *Kit*$^{W\text{-}sh/W\text{-}sh}$ mice (Fig. S5A). Despite a role for mast cells and sensory neurons in promoting each others' responses (Azimi et al., 2017; Green et al., 2019; Meixiong et al., 2019a; Serhan et al., 2019), we found no effect of mast cell deficiency on papain-induced SP release from skin explants or DRG cultures (Fig. S5B–C). Similarly, we found no difference in the percentage or number of activated (PDL2$^+$) CD301b$^+$ DCs in the dLN 24 hours after papain-immunization in wild type or *Kit*$^{W\text{-}sh/W\text{-}sh}$ mice (Fig. S5D). These data indicate that *Kit*-independent neuronal activation, but not mast cell activation, is required for SP release and CD301b$^+$ DC migration.

Substance P acts through MRGPRA1 on CD301b$^+$ DCs to promote their migration

SP is a cationic neuropeptide that binds to its classical receptors TACR1 and TACR2 as well as the Mas-related G protein coupled receptors MRGPRA1 and MRGPRB2 in the mouse (Azimi et al., 2017; Azimi et al., 2016; McNeil et al., 2015). Using the Immgen database we found low, but detectable expression of *Tacr1* and *Tacr2* in all cutaneous DC subsets and no detectable expression of *Mrgprb2* (Fig. S6A). *Mrgpra1* transcript could be detected in the Langerin$^-$CD103$^-$CD11b$^+$ DC subset, which contains the dermal CD301b$^+$ DCs (Fig. S6A). To confirm these findings, we performed qPCR of bulk BMDCs, which are largely composed of the cDC2s (Gao et al., 2013). BMDCs expressed *Mrgpra1*, but not other known receptors for SP (Fig. 6A). To verify this expression on in vivo CD301b$^+$ DCs, we sorted CD301b$^+$ DCs and CD103$^+$ DCs from the dLN after papain immunization. We could not reliably detect *Tacr1* or *Tacr2* on either DC subset (Fig. S6B). However, CD301b$^+$ DCs, but not CD103$^+$ DCs, expressed *Mrgpra1* indicating that CD301b$^+$ DCs may be specifically sensitive to the effects of SP (Fig. 6B). In order to determine the role of MRGRPA1, we sought to block its function using chemical antagonists. Specific antagonists of MRGPRA1 have not been described, so to determine the effects of MRGPRA1 blockade we compared the effect of the peptide antagonist QWF which blocks TACR1, TACR2, MRGPRB2, and MRGPRA1 to the small molecular antagonist L733060 which only blocks TACR1, TACR2, and MRGPRB2 (Azimi et al., 2017; Azimi et al., 2016). Consistent with a role for MRGPRA1 in CD301b$^+$ DC migration, co-immunization with QWF, but not L733060, led to a defect in papain-induced CD301b$^+$ DC migration (Fig. 6C).

To this point our data suggested that SP acts through MRGPRA1, expressed on CD301b$^+$ DCs, to promote the allergen-induced migration of CD301b$^+$ DCs. This effect appeared to be independent of SP-induced CCR7 upregulation (Fig. 6D), but to confirm the role of *Mrgpra1* in allergen-induced CD301b$^+$ DC migration in vivo we generated mixed BM chimeras. We transferred an equal ratio of wild type and *Cd301b*^{DTR} or *Mrgpra1*$^{-/-}$ and *Cd301b*^{DTR} BM into lethally irradiated wild type recipients to generate CD301b^{WT} and

CD301b$^{Mrgpra1-/-}$ chimeras, respectively (Fig. 6E). After reconstitution, both groups were treated with DT to yield mice with wild type sensory neurons, mixed CD45$^+$ immune cell compartments, and either *Mrgpra1* sufficient (CD301b^{WT}) or deficient (CD301b$^{Mrgpra1-/-}$) CD301b$^+$ DCs (Fig. 6E). Consistent with a requirement for *Mrgpra1* in allergen-induced CD301b$^+$ DC migration, papain-induced CD301b$^+$ DC migration was lost in CD301b$^{Mrgpra1-/-}$ chimeras (Fig. 6F). In order to directly compare the migration of *Mrgpra1* sufficient or deficient CD301b$^+$ DCs in vivo, we made additional chimeras in which lethally irradiated wild type mice were reconstituted with an equal ratio of CD45.1$^+$ wild type BM and CD45.2$^+$ *Mrgpra1*$^{-/-}$ BM. We compared the ratio of wild type versus *Mrgpra1*$^{-/-}$ CD301b$^+$ DCs in the naïve skin to that in the dLN after papain immunization and found that wild type DCs displayed a significant advantage in allergen-induced migration to the dLN (Fig. 6G). This wild type advantage was lost when examining CD103$^+$ DC migration in response to LPS immunization (Fig. 6H), indicating that *Mrgpra1* plays a crucial role in the allergen-induced migration of CD301b$^+$ DCs.

CD301b$^+$ DCs require CCR7 to enter the draining lymphatics and then CCR7 and CCR8 to cross the subcapsular sinus and enter the dLN parenchyma (Sokol et al., 2018). Because CD301b$^+$ DCs do not upregulate CCR7 expression upon allergen immunization, it has remained unclear how CD301b$^+$ DCs are signaled to leave the skin parenchyma to migrate to the draining lymphatic vessels (Sokol et al., 2018). Stimulation with SP or the MRGPRA1 agonist FMRF induced BMDC chemokinesis across a Transwell membrane in the absence of any chemokine gradient (Fig. 6I) (Liu et al., 2009). Furthermore, BMDCs stimulated with SP or FMRF exhibited augmented migration to the CCR7 ligand CCL21 (Fig. 6J). The effect of SP on chemokinesis and chemotaxis was lost in BMDCs from *Mrgpra1*$^{-/-}$ mice, indicating that SP promotes DC migration through MRGPRA1 (Fig. 6K and L) (Meixiong et al., 2019b).

TRPV1$^+$ neurons are required for Th2 cell differentiation in response to papain

CD301b$^+$ DCs are necessary for Th2 cell differentiation in response to cutaneous allergens and disruption of their migration into the parenchyma of the dLN blocks Th2 cell differentiation in response to papain (Kumamoto et al., 2013; Sokol et al., 2018). Consistent with their role in allergen-induced CD301b$^+$ DC migration, we found that depletion of *Trpv1*$^+$ neurons led to decreased allergen-induced Th2 cell differentiation (Fig. 7A and B). CD4$^+$ T cells expressed significantly less IL-4 (Fig. 7C) and IL-13 (Fig. 7D), indicating a block in Th2 cell differentiation. There was no concurrent increase in IFNγ production by CD4$^+$ T cells, suggesting that this block was related to CD4$^+$ T cell activation and not Th2 cell polarization (Fig. 7E). Consistent with this, we found a decrease in the percentage of activated CD44^{high} CD4$^+$ T cells in mice depleted of *Trpv1*$^+$ neurons (Fig. 7F). Similarly, using IL-4-eGFP mice (4get) we found that co-immunization of OVA and papain together with QX314 or QWF inhibited the production of IL-4-eGFP$^+$ and activated CD44^{high} and CD69^{high} CD4$^+$ cells as compared to OVA and papain alone (Fig. 7G and H) (Mohrs et al., 2001). These data suggest that blocking the allergen-induced and *Trpv1*-dependent migration of CD301b$^+$ DCs leads to defective CD4$^+$ T cell activation and Th2 cell differentiation that is secondary to decreased lymph node entry of CD301b$^+$ DCs. Finally, although SP-induced DC migration was necessary for Th2 cell differentiation, it was not

sufficient, indicating that an additional signal or cell is required to promote Th2 cell differentiation in vivo (Fig. 7G).

DISCUSSION

In the classical PAMP-PRR signaling paradigm, tissue DCs act as direct sensors of Type-1 immunogens such as bacteria and viruses to initiate adaptive immune responses (Iwasaki and Medzhitov, 2015). Here we have shown that this paradigm may not be applicable to Type-2 (allergic) immunity. We found that TRPV1$^+$ neurons acted as the primary allergen sensor, eliciting the sensation of itch and pain and the release of SP upon exposure. SP then stimulates proximally located Th2 cell-skewing CD301b$^+$ DCs through MRGPRA1 to promote their movement. Activation of sensory neurons was necessary for the initiation of Th2 cell differentiation. We propose that DCs do not directly sense allergens and instead require the initial activation of a primary sensor. In the case of proteolytically active allergens such as papain, HDM, or Alternaria, the sensory nervous system acts as that primary sensor of allergen exposure to initiate the adaptive Type-2 immune response. IL-4 and IL-13, produced in the context of chronic allergic inflammation can decrease the activation threshold of itch sensing neurons, which could link allergen-induced acute activation of the sensory nervous system with chronic allergic inflammation (Oetjen et al., 2017).

Our study revealed that SP acts through MRGPRA1 to induce the migration of CD301b$^+$ DCs to the dLN. Importantly, SP induced migration was not sufficient for Th2 cell differentiation. This is consistent with studies showing an important role for innate alarmins in Th2 cell differentiation and allergic inflammation, but only a partial role in DC migration (Besnard et al., 2011; Cayrol et al., 2018; Palm et al., 2013). Both signals may be required to fully license the DC to promote Th2 cell differentiation, or they may individually act on DCs and putative accessory cells that provide the necessary skewing information for Th2 cell differentiation (Halim et al., 2018). This two-signal requirement could be essential to reduce the risk of non-specific or bystander activation of DCs. Unlike PAMPs, which DCs normally interact with in the context of antigens, indirect activation of DCs by neurons separates the activation trigger from the antigen. If both sensory neuron activation and alarmins are required for full DC licensing, this may limit DC activation to those DCs in areas of high antigen concentration. However, this separation of antigen from adjuvant detection runs the risk of activating DCs presenting bystander antigens and could underlie the clinical observation of “allergen creep” in which atopic individuals progressively gain additional allergen sensitizations (Brough et al., 2015; Migueres et al., 2014).

Why is SP required for DC migration in the Type-2 immune response? Unlike in the PAMP-PRR signaling paradigm, DCs fail to directly sense allergen-associated molecular patterns and do not upregulate CCR7 upon allergen exposure. We propose that the SP signal is necessary to induce chemokinesis, allowing Th2 cell skewing CD301b$^+$ DCs to release contacts from within the dermis. How SP induces chemokinesis is unknown, but it is possible that MRGRPA1 signaling promotes Src phosphorylation, which we and others have shown to be necessary for optimal DC migration (Hauser et al., 2016; Sokol et al., 2018). Unanchored CD301b$^+$ DCs can then utilize their baseline expression of CCR7, which is

necessary for their migration into draining lymphatics, to sense and respond to homeostatic CCL21 gradients and migrate to the dLN (Ohl et al., 2004; Sokol et al., 2018). This provides a potential mechanism by which allergen-activated DCs – in contrast to mast cells that can directly respond to allergens through IgE cross-linking – are able to sense and migrate out of the peripheral tissues without direct allergen detection and without concomitant upregulation of CCR7 (Lin et al., 2018). It also raises an important question as to why cDC2s are specifically required for Th2 cell differentiation. cDC2s may provide unique Th2 cell skewing signals in the dLN or they may act upon sensory neurons in the skin to promote their activation (Xu et al., 2020). Alternatively, could cDC2s be required for Th2 cell differentiation simply because their expression of *Mrgpra1* endows them with the unique ability to migrate to the dLN in response to allergen exposure? If so, forced expression of *Mrgpra1* on different DC subsets should be sufficient to endow other DCs with Th2 cell skewing capability.

Cysteine protease allergens, including papain and HDM, induce Ca^{2+} flux of DRG neurons in culture which indicates that nociceptive neurons directly sense allergens (Reddy et al., 2015; Serhan et al., 2019). How this sensing occurs is unclear. Protease activated receptors (PARs) 2 and 4 are cleaved by papain and have been associated with the itch response, but the interpretation of some of these studies is complicated by the fact that the PAR2 agonist SLIGRL also activates MRGPRC11 to mediate itch (Liu et al., 2011). Indeed, the MRGPR family plays a major role in neuronal itch sensing, with MRGPRA3 mediating chloroquine induced itch and MRGPRA1 mediating bilirubin induced itch (Liu et al., 2009; Meixiong et al., 2019b). MRGPRs are expressed on both mast cells and sensory neurons, permitting these cells to directly communicate through the release of preformed mediators including neuropeptides to promote itch and allergic inflammation (Meixiong et al., 2019a; Serhan et al., 2019). Here we found that $CD301b^+$ DCs expressed MRGPRA1, but not other SP receptors. This may permit $CD301b^+$ DC migration to be directly activated by MRGPRA1 agonists, such as bilirubin (Meixiong et al., 2019b). We found that $CD301b^+$ DC expression of MRGPRA1 allowed them to sense SP from sensory neurons and migrate in response to allergen exposure, although this data from mixed BM chimeras will ultimately need to be confirmed using a model in which *Mrgpra1* is specifically ablated in $CD301b^+$ DCs. This may also permit $CD301b^+$ DC migration to be directly activated by MRGPRA1 agonists, such as bilirubin (Meixiong et al., 2019b). Our data is in contrast to reports showing that various DC subsets express *Tacr1* and respond to SP and its analogues by promoting DC survival and migration, as well as skewed Th1 cell and cytotoxic T cell responses (Janelsins et al., 2009; Janelsins et al., 2013; Mathers et al., 2007). We did not detect *Tacr1* in $CD301b^+$ DCs, but it is possible that differential expression of SP receptors by DC subsets could lead to different functional outcomes. Ultimately, this communication between the sensory nervous system and immune cells could be a rapid way to initiate protective host defenses (Cohen et al., 2019; Kashem et al., 2015), but its dysregulation could drive inflammatory or allergic diseases (Riol-Blanco et al., 2014; Talbot et al., 2015; Trankner et al., 2014).

The critical role of $TRPV1^+$ sensory neurons and SP-driven DC migration in the development of allergic immune responses to cutaneous allergens provides a targetable pathway for the prevention and treatment of allergic diseases. $TRPV1^+$ neurons activated optogenetically or by *Candida* infection release CGRP that promotes activation of the IL-17-

mediated anti-fungal immune response (Cohen et al., 2019; Kashem et al., 2015). How *Candida* can promote CGRP release while protease allergens induce SP release is unclear. While *Candida* and protease allergens may activate different subsets of TRPV1$^+$ neurons, TRPV1$^+$ neurons may also be able to differentiate between stimuli to promote different immune responses through unique neuropeptide release patterns. CGRP release may specifically induce innate IL-17 related inflammatory responses while SP may specifically induce initiation of the Type-2 adaptive immune response. SP has already been shown to directly activate mast cells through MRGPRB2 (Serhan et al., 2019), could SP act as a master regulator of innate Type-2 immune cells? The full extent of how CGRP and SP specifically activate different arms of Th-mediated immunity remain unclear, however exploiting the neuropeptide specificity for initiating Type-1, Type-2, and Type-17 immune responses would allow for targeted therapeutics. The TACR1 antagonist serlopitant has recently been shown to be effective in the treatment of chronic itch (Yosipovitch et al., 2018). Although our data suggest that TACR1 antagonists are unlikely to alter CD301b$^+$ DC migration, drugs that target MRGPRX2, the human orthologue of MRGPRA1, may be targets for allergic diseases. Conversely, many common drugs act as MRGPRX2 agonists (McNeil et al., 2015). Whether this leads to DC migration and allergic sensitization in humans remains unknown. But together, these data establish mechanisms for DC migration in allergic immune responses which may be applied to the prevention and treatment of allergic diseases.

STAR METHODS

RESOURCE AVAILABILITY

Lead contact: Further information and requests for resources and reagents should be directed to and will be fulfilled by the Lead Contact, Caroline L. Sokol (CLSOKOL@mgh.harvard.edu).

Materials Availability: This study did not generate new unique reagents or animal strains.

Data and Code Availability—This study did not generate any unique datasets or code.

EXPERIMENTAL MODEL AND SUBJECT DETAILS

Mice: All animal experiments were approved by the Massachusetts General Hospital or Harvard Medical School Institutional Animal Care and Use Committee (IACUC). Mice were bred and maintained in a specific-pathogen-free (SPF) animal facility at Massachusetts General Hospital. C57BL/6, *Kit*$^{W\text{-}sh/W\text{-}sh}$, Ly5.1, and *Tac1*$^{-/-}$ mice were purchased from Charles River Laboratories (Wilmington, MA) or Jackson Laboratories (Bar Harbor, ME). *Nav1.8*^{cre} mice were originally from Dr. John Wood (University College London), and Trpv1^{DTR} from Dr. Mark Hoon (NIH). Kaede mice were originally from Osami Kanagawa and were crossed with *Trpv1*^{DTR} mice to generate Kaede *x Trpv1*^{DTR} mice. *Nav1.8*^{cre} mice were crossed with *tdTomato*^{loxSTOPlox} to generate *Nav1.8*^{tdTomato} mice. 4get mice on a C57BL/6 background were provided by Markus Mohrs. Bone marrow from *Mrgpra1*$^{-/-}$mice on a C57BL/6 background was kindly provided by Dr. Xinzhong Dong (Johns Hopkins, MD). Mice were used in experiments at 5–14 weeks of age. Sex and age-matched littermates

or purchased C57Bl/6 mice were used as wild type controls. Both female and male mice were used for all experiments and numbers were matched among the experimental conditions.

Experimental mouse models:

Diphtheria Toxin Depletion: C57Bl/6, *Trpv1*^{DTR}, Kaede, or Kaede x *Trpv1*^{DTR} mice were injected intraperitoneally (i.p) with 0.2 μg of DT (Sigma-Aldrich) daily for 5 days then rested for 2 days repeated over a 21 day period. Mice rested for seven days post final DT injection. Effective depletion was confirmed through tail flick assay, and qPCR of DRGs. For the tail flick assay, the tail of each mouse was placed into 52°C water for a maximum of ten seconds, or less if mouse removed the tail from water. For CD301b+ DC depletion in epicutanous immunization experiments, following depilation of fur on the tail flank skin of wild type and *Cd301b*^{DTR} mice, 0.5 μg of DT in 100 μl PBS was injected intraperitoneally for three consecutive days. The epicutaneous patch was applied on the third day of DT injections. For BM chimera experiments, mice were injected with 0.5 μg of DT in 100 μl PBS on two consecutive days. On the second day of DT injection, mice were also immunized with OVA or OVA & papain, then euthanized 24 hours later for analysis of DC migration.

Kaede Photoconversion: A 2 × 2 cm patch of skin above the base of tail was shaved followed by application of a chemical depilatory agent (Veet) for 1 min, then removed by multiple washings with PBS. The exposed skin was subjected to violet light (420 nm) using a Bluewave LED visible light curing unit (Dymax) with a 420 nm bandpass filter (Andover Corp). Skin was exposed to this wavelength with the light source at a maximum power, approximately 7.5 cm away from the skin for 5 min. Following photoconversion, mice were immunized intradermally or epicutaneously in the shaved region as described above. 24 hours following immunization, dLNs were isolated and analyzed for skin DC migration using flow cytometry.

Bone marrow chimera generation: Donor bone marrow (BM) was extracted from femurs and tibias of donor mice using a mortar and pestle. RBCs were lysed, then the purified BM cells were resuspended in 1xPBS. 10×10^6 BM cells in 100 μL of PBS were intravenously injected into lethally irradiated (1000 rads) C57Bl/6 recipients within 3 hours of irradiation. For comparative migration experiments, recipient WT mice received a 1:1 mix of WT/*CD301b*^{DTR} BM (CD301b^{WT} mice) or *Mrgpra1*$^{-/-}$/*CD301b*^{DTR} BM (CD301b$^{Mrgpra1-/-}$ mice). Recipient mice were rested for 6–8 weeks, then injected intraperitoneally with 0.5 μg diphtheria toxin (DT). 24 hours later, mice were again injected intraperitoneally with 0.5 μg DT followed by intradermal footpad injections with 50 μg OVA in the right footpad and 50 μg OVA + 50 μg papain in the other footpad. 24 hours later, the dLN was harvested for assessment of CD301b$^+$ DCs by flow cytometry. For competitive migration experiments, recipient WT mice received a 1:1 mix of CD45.1 WT/CD45.2 *Mrgpra1*$^{-/-}$ BM. Recipient mice were rested for 6–8 weeks, then intradermally injected with 50 μg OVA + 50 μg papain or 50 μg OVA + 10 μg LPS in bilateral footpads. 24 hours later, the dLN and ear skin was harvested for chimeric assessment of CD11c$^+$CD301b$^+$ DCs (OVA & papain) or CD11c$^+$CD103$^+$ DCs (OVA & LPS) by flow cytometry.

Cell or tissue isolation and culture: Both female and male mice were used for all cell and tissue culture experiments and numbers were matched among the experimental conditions.

Dorsal Root Ganglia Cultures and Stimulation: Dorsal root ganglia (DRGs) were harvested from mice (7–14 weeks old) and dissected into DMEM supplemented with 0.1% glucose, 0.1% L-glutamine, 0.1% sodium pyruvate (Corning) with added 10% heat inactivated FBS (Sigma-Aldrich) and 1% Pen/Strep (Lonza). DRGs were then dissociated in 1.25 mg/mL Collagenase A (Roche) + 2.5 mg/ml Dispase II (Sigma-Aldrich) in 1x PBS (Corning). Dissociated DRGs were washed in supplemented DMEM and were triturated using needles of different sizes (18G, 21G, 26G, six times each) in Neurobasal-A medium (Invitrogen) supplemented with B27 (Invitrogen), 1% GlutaMAX™, and 1% Pen/Strep, with added growth factors 0.01 mM arabinocytidine (Ara-C), 0.002 ng/μL glial derived neurotrophic factor (GDNF) (Sigma-Aldrich) and nerve growth factor 2.5S (NGF 2.5S) (Invitrogen). For culture in a 96-well sterile tissue-culture (TC) treated plate (Corning), around 12,000 DRG neurons/well were plated at a standard 30 μL/well into 10 μg/ml laminin (Sigma-Aldrich) pre-coated plates and incubated for one hour at 37°C in a CO_2 tissue incubator (Thermo Scientific). After the one-hour incubation, 100 μL of supplemented Neurobasal-A medium with added growth factors was added to each well. The DRGs incubated for 24 hours. For stimulations, media was replaced with 200 μL/well of supplemented Neurobasal-A medium without the addition of growth factors and DRG neuron cultures were either left unstimulated with vehicle control (PBS) or stimulated with papain, heat-inactivated papain, increasing concentrations (100 μg/mL, 150 μg/mL, or 200 μg/mL) of Alternaria extract or HDM extract for 1 hour. Supernatant was used for further analysis.

Flank Explant Assay: Wild type mice were shaved at the flanks and injected as described. Mice were immediately sacrificed and punch biopsies of the shaved flanks were collected and rapidly transferred into a 24-well plate containing 1mL of serum free DMEM. Explants were incubated for 30 min at 32 °C with gentle rotation (150 rpm) before supernatants were collected for analysis.

Generation of Bone Marrow-derived Dendritic Cells (BMDCs): BM was harvested from 5- to 8-week-old mice by mechanical disruption using a mortar and pestle, followed by incubation with red blood cell lysis buffer (Sigma-Aldrich). BM cells were cultured in growth media supplemented with 10% HI FBS (Sigma-Aldrich), 1% Pen/Strep (Lonza), 1% GlutaMAX™(Gibco), 1% HEPES buffer (Corning), 1% Non-Essential Amino Acid Solution (Lonza), 1% Sodium Pyruvate (Gibco), 0.1% 2-mercaptoethanol (Gibco), with 20 ng/mL of granulocyte-macrophage colony-stimulating factor (GM-CSF) (Peprotech) at a density of 0.7×10^6 cells/mL, fed on days 2 and 4 and stimulated on day 5 of culture.

Stimulation of Primary Dendritic Cells: Skin draining lymph nodes from naïve C57Bl/6 mice were harvested and digested as described in *Flow cytometry and Cell sorting*. Cell suspensions underwent MACS-mediated CD11c positive selections (Miltenyi) followed by overnight stimulation with heat inactivated papain (100 μg/ml), papain (100 μg/ml), or LPS

(100 ng/ml) at 1×10^6 cells per ml in fully supplemented RPMI with 10% heat inactivated fetal bovine serum. Cells were harvested and processed for flow cytometric analysis.

METHOD DETAILS

Intradermal Immunizations: Mice were immunized intradermally (i.d) in the right side of the cheek (behavioral experiments), base of tail (Kaede experiments), or in footpads. As indicated, mice were immunized with 50 μg of papain, heat-inactivated papain, ovalbumin, histamine, or 40 μg of Capsaicin (all from Sigma-Aldrich); or 100 μg of Alternaria alternata (Greer). Where indicated, mice were injected with 10 μg LPS (InvivoGen), 5 μg CGRP (Sigma-Aldrich), 100 nmoles Substance P (Tocris) or 1% QX314 (Tocris). All dilutions were diluted in sterile 1x phosphate buffered saline, or PBS (Corning), except for capsaicin which was diluted in PBS and 6.4% DMSO. Where indicated, immunizations were performed with either 500 μmol of QWF or L733060 (both from Tocris) diluted in a 5% DMSO PBS solution.

Epicutaneous sensitization: Mice were shaved and depilated (Veet) on their back two days before a 1cm x 1cm gauze soaked in 100 μl of 2 mg/ml OVA in PBS, Papain in PBS, or PBS alone was placed on the back skin near the base of the tail and covered with a waterproof transparent adhesive film (Flexigrid, Smith and Nephew Opsite) for 24 hours.

Behavioral Analysis: For pain and itch assays, mice were allowed to acclimate to cage apparatus for two hours prior to filming, with food and water provided. A white noise machine (Marpac) was used to reduce distractions from behavioral response. After habituation, mice were immunized i.d. in the right cheek with allergen administered in a 25 μL vehicle under brief isoflurane anesthesia. Mice were videotaped in isolation for 20 minutes. Videos were then examined for quantification of wiping (single ipsilateral paw to injected cheek) and scratching (ipsilateral hind paw to injected cheek). Data was quantified in five-minute intervals.

Calcium Imaging of DRG Neuronal Cultures: DRGs were harvested and digested in a mix of Collagenase A (2.5 mg/ml) and Dispase II (1 mg/mL) for 80 min while shaking at 37°C, DRGs were then resuspended in DMEM/F12 (Thermo Fisher) and mechanically triturated using needles of different sizes (18G, 21G, 26G, six times each). The cell suspension was carefully plated on laminin precoated 35 mm plates in DMEM/F12 supplemented with NGF 25 ng/mL and GDNF 2 ng/mL and cultured overnight.

For calcium imaging, cells were loaded with 5 μM Fura-2-AM / DMEM/F12 (Thermo Fisher) at 37°C for 30 min, washed 3x, and imaged in 2 mL Krebs-Ringer solution (Boston Bioproducts) (KR: 120 mM NaCl, 5 mM KCl, 2 mM $CaCl_2$, 1 mM $MgCl_2$, 25 mM sodium bicarbonate, 5.5 mM HEPES, 1 mM D-glucose, pH 7.2 ± 0.15). 100 μg Papain or Vehicle (PBS) stimulation were followed by 100 μM histamine, 1 mM chloroquine, 1 μM capsaicin and 80 mM KCl sequentially application to identify shared neuronal responses of itch sensitizing stimulants with each other and $TRPV1^+$ neurons. Images were acquired with alternating 340/380 nm excitation wavelengths, and fluorescence emission was captured using a Nikon Eclipse Ti inverted microscope and Zyla sCMOS camera (Andor).

Ratiometric analysis of 340/380 signal intensities were processed, background corrected, and analyzed with NIS-elements software (Nikon) by drawing regions of interest (ROI) around individual cells as also previously described (Lai et al., 2019).

Each neuron was analyzed for excitability with an increase from baseline greater than 15% was considered to be a positive response. All neurons responding to KCl are considered viable and potentially excitable. With that as a baseline, the subsequent percentages of papain, histamine, chloroquine, capsaicin, and vehicle responsive cells were quantified and plotted as proportion of KCI responsive cells. Response traces of single DRG neurons were generated using Microsoft Excel. Venn Diagram showing the numbers of individual neurons responding one or more stimulants was created using R studio 3.6.2. Violin plots were created using GraphPad PRISM software 8.4.

Microscopy and Image Quantification: Ears were harvested, split into dorsal and ventral halves, removed of hair (Veet) and placed on Flexigrid™ transparent adhesive film (Smith and Nephew Opsite) dermal side up. Fat was gently removed and each tissue sample was floated on 3 mL of DMEM (Corning) supplemented with 3 mg/mL Dispase II (Sigma-Aldrich) per well of a 6-well plate, dermal side down, for 90 minutes at 37°C in 5% CO_2. Afterwards, the samples were dried and the dermal tissue was gently peeled away from the epidermal tissue. Dermal slices were then isolated, rinsed in PBS, and fixed in a 4% paraformaldehyde (Electron Microscopy Sciences) PBS solution for 1 hour at 4 °C. After washing in PBS, samples were incubated overnight with a primary antibody solution of biotinylated anti-Tuj1 (BD Biosciences) diluted in PBS with 0.2% TritonX-100 (Sigma-Aldrich) and 10% heat inactivated goat serum (Jackson ImmunoResearch). Samples were washed 3 times for 10 min in PBS with 0.2% TritonX-100 and 2% heat inactivated goat serum and then stained with Streptavidin-AF488, CD301b-AF647, and MHCII-BV421 (all from BioLegend) diluted in PBS with 0.2% TritonX-100 and 10% heat inactivated goat serum for 1 hour at room temperature with shaking. Washed ears were mounted using Prolong Diamond Antifade Mountant (Thermo Fisher Scientific) prior to imaging on a Zeiss LSM confocal microscope. Images were analyzed using Zen Blue to quantify the distance of $MHCII^+CD301b^+$ cells and $MHCII^+CD301b^-$ cells from their nearest $Nav1.8^+$ neuron as measured in 3D Ortho.

Enzyme-Linked Immunosorbent Assay (ELISA): Mouse Substance P and CGRP were detected using competitive mouse Substance P and CGRP ELISA kits (both from Cayman Chemical). All procedures were carried out according to the manufacturer's protocols. Samples were assayed on Softmax Pro Software in duplicates and concentrations were determined from a standard curve.

Flow Cytometry and Cell Sorting: Harvested lymph nodes were subjected to digestion at 37°C in DNase I (100 μg/mL, Roche), Collagenase P (200 μg/mL, Sigma-Aldrich), Dispase II (800 μg/mL, Sigma-Aldrich), and 1% fetal calf serum (FCS) in RPMI. At 7 min intervals, supernatant was removed and replaced with fresh enzyme media until no tissue fragments remained. Supernatant was added to added to stop buffer (RPMI/2mM EDTA (Gibco)/1% FBS) and filtered prior to antibody staining. To analyze the cells of skin, ears was harvested and forceps were used to separate the dorsal and ventral halves. The

epidermis was attached to Flexigrid™ transparent adhesive film (Smith and Nephew Opsite), then ear halves were floated dermis side down in Dispase II (3 mg/mL, Sigma-Aldrich) in DMEM for 90 minutes at 37°C in 5% CO_2. The dermis was then removed from the epidermis, which remained on the Flexigrid™ tape. The epidermis was digested in Collagenase IV (2 mg/mL, Sigma-Aldrich) in DMEM, while the dermis was digested in Liberase TM (25 μg/mL, Sigma-Aldrich), DNAse I (75 μg/mL, Sigma-Aldrich), and 10 μM HEPES (Corning) in DMEM. The dermis and epidermis were digested for 45 minutes at 37°C in 5% CO_2; tubes containing the dermal and epidermal samples were vigorously shaken every 9 minutes. Following digestion, 500 μL of 15 μM EDTA (Gibco) in heat inactivated FBS (Sigma-Aldrich) was added to each sample. The dermis was subjected to gentleMACS dissociation, then dermal and epidermal cell suspensions were combined and filtered before antibody staining. Enzymatically digested cell suspensions were incubated for 15 min at 4°C in PBS with 0.5% FCS with the following antibodies: anti-CD16/CD32, anti-CD11b, anti-CD11c, anti-CD103, anti-CD301b, anti-CD4, and anti-PDL2 (all from BioLegend). Intracellular cytokine staining was performed after PMA/Ionomycin (Sigma) stimulation of single cell suspensions in the presence of GolgiPlug for 4 hours prior to intracellular staining using BD Cytofix/Cytoperm kit (BD Biosciences). Viability was determined using Fixable Viability Dye eFluor 780 (Invitrogen). Samples were run on Beckman Coulter's CytoFLEX S, BD Fortessa X20 or BD FACSAria Fusion and analyzed using FlowJo (Version 10) (TreeStar).

Quantitative PCR (qPCR): Total RNA from sorted cells, DRGs, or BMDCs was isolated using the QIAGEN RNeasy Micro Kit in accordance with the manufacturer's protocol. 50 μL of cDNA per reaction was generated using random hexamers, Oligo (dT), magnesium chloride, dNTPs (10 mM), Reverse Transcriptase, and RNase inhibitor (all from Thermo Fisher Scientific). A Roche LightCycler 96 Real-Time PCR System was utilized to quantify gene expression, with SYBR Green Master Mix (Roche). The reaction cycles were: 95°C for 600 s, then 95°C, 60°C, and 72°C for 10 s each for 45 total cycles, followed by 95°C for 10 s, 65°C for 60 s, and finally 97°C for 1 s. Fluorescence was quantified during each amplification. Quantification cycle (Cq) values for each sample were determined using Roche LightCycler 96 Software 1.1. Microsoft Excel was used to determine copy values for Cq in order to divide by *Gapdh* copy values for ratio analysis.

Chemotaxis Assays: On day 5 of culture, BMDCs were stimulated with: LPS (100 ng/mL, InvivoGen), papain (100 μg/mL, Sigma-Aldrich), Substance P (0.5 μM, Sigma-Aldrich), Nle-Arg-Phe amide, or FMRF (30 μM, Sigma-Aldrich). Cells were then harvested. Chemotaxis was performed on these harvested cells using 5 μm pore size Transwell membranes (NeuroProbe). 32 μL of CCL21 (100 ng/mL) or media alone with 0.5% BSA in RPMI, were added to the wells of the lower chamber. The Transwell membrane was then outfitted to the microplate, after which 100,000 cells in 50 μL of chemotaxis media were added in triplicate. Plates were incubated for 2 hr at 37° C in 5% CO_2. Afterwards, the membrane was quickly rinsed with sterile PBS and spun down for one minute at 1500 rpm to collect any migrated adherent cells. The membrane was then removed, and migrated cells were counted.

QUANTIFICATION AND STATISTICAL ANALYSIS

Statistical analysis of results was performed using GraphPad Prism 7–8 (GraphPad Software). Unpaired t-test or ordinary one-way ANOVA were applied as indicated in figure legends. Statistical significance was considered for P *values* <0.05. Details are listed in the respective figure legends.

Supplementary Material

Refer to Web version on PubMed Central for supplementary material.

ACKNOWLEDGEMENTS

This work was supported by K08AI121421 (C.L.S), DP2AT009499 (I.M.C.), R01AI130019 (I.M.C.), T32HL116275 (C.H.F.), DFG PE2864/3-1 (C.P.), Center for the Study of Inflammatory Bowel Disease Pilot Feasibility Study Award DK043351 (C.L.S.), Massachusetts General Hospital Transformative Scholar Award (C.L.S.), AAAAI Foundation and Dr. Donald Y. M. Leung/JACI Editors Faculty Development Award (C.L.S.), Food Allergy Science Initiative (C.L.S. and I.M.C.). I.M.C. receives additional support from the Chan-Zuckerberg Initiative, Burroughs Wellcome Fund, Harvard Stem Cell Institute, GlaxoSmithKline (GSK), Allergan Pharmaceuticals. Cytometric findings reported here were performed in the MGH Department of Pathology Flow and Image Cytometry Research Core, with support from the NIH Shared Instrumentation Program (1S10OD012027-01A1, 1S10OD016372-01, 1S10RR020936-01, and 1S10RR023440-01A1). We thank N. Andrew (MGH) for technical advice, M. Hoon (NIH) for providing $Trpv1^{DTR}$ mice, K. Blake and S. Sannajust (Harvard) for breeding $Tac1^{-/-}$, $Nav1.8^{cre}$ and $tdTomato^{loxSTOPlox}$ mice, X. Dong (Johns Hopkins) for providing $Mrgpra1^{-/-}$ bone marrow. BioRender.com was used to produce the graphical abstract.

REFERENCES

Azimi E, Reddy VB, Pereira PJS, Talbot S, Woolf CJ, and Lerner EA (2017). Substance P activates Mas-related G protein-coupled receptors to induce itch. J Allergy Clin Immunol 140, 447–453 e443. [PubMed: 28219706]

Azimi E, Reddy VB, Shade KC, Anthony RM, Talbot S, Pereira PJS, and Lerner EA (2016). Dual action of neurokinin-1 antagonists on Mas-related GPCRs. JCI Insight 1, e89362. [PubMed: 27734033]

Baral P, Umans BD, Li L, Wallrapp A, Bist M, Kirschbaum T, Wei Y, Zhou Y, Kuchroo VK, Burkett PR, et al. (2018). Nociceptor sensory neurons suppress neutrophil and gammadelta T cell responses in bacterial lung infections and lethal pneumonia. Nat Med 24, 417–426. [PubMed: 29505031]

Besnard AG, Togbe D, Guillou N, Erard F, Quesniaux V, and Ryffel B (2011). IL-33-activated dendritic cells are critical for allergic airway inflammation. Eur J Immunol 41, 1675–1686. [PubMed: 21469105]

Binshtok AM, Bean BP, and Woolf CJ (2007). Inhibition of nociceptors by TRPV1-mediated entry of impermeant sodium channel blockers. Nature 449, 607–610. [PubMed: 17914397]

Brough HA, Liu AH, Sicherer S, Makinson K, Douiri A, Brown SJ, Stephens AC, Irwin McLean WH, Turcanu V, Wood RA, et al. (2015). Atopic dermatitis increases the effect of exposure to peanut antigen in dust on peanut sensitization and likely peanut allergy. J Allergy Clin Immunol 135, 164–170. [PubMed: 25457149]

Cayrol C, Duval A, Schmitt P, Roga S, Camus M, Stella A, Burlet-Schiltz O, Gonzalez-de-Peredo A, and Girard JP (2018). Environmental allergens induce allergic inflammation through proteolytic maturation of IL-33. Nature immunology 19, 375–385. [PubMed: 29556000]

Chen J, and Lariviere WR (2010). The nociceptive and anti-nociceptive effects of bee venom injection and therapy: a double-edged sword. Prog Neurobiol 92, 151–183. [PubMed: 20558236]

Chiu IM, Heesters BA, Ghasemlou N, Von Hehn CA, Zhao F, Tran J, Wainger B, Strominger A, Muralidharan S, Horswill AR, et al. (2013). Bacteria activate sensory neurons that modulate pain and inflammation. Nature 501, 52–57. [PubMed: 23965627]

Choi HW, Suwanpradid J, Kim IH, Staats HF, Haniffa M, MacLeod AS, and Abraham SN (2018). Perivascular dendritic cells elicit anaphylaxis by relaying allergens to mast cells via microvesicles. Science 362.

Cohen JA, Edwards TN, Liu AW, Hirai T, Jones MR, Wu J, Li Y, Zhang S, Ho J, Davis BM, et al. (2019). Cutaneous TRPV1(+) Neurons Trigger Protective Innate Type 17 Anticipatory Immunity. Cell 178, 919–932 e914. [PubMed: 31353219]

Dawicki W, Jawdat DW, Xu N, and Marshall JS (2010). Mast cells, histamine, and IL-6 regulate the selective influx of dendritic cell subsets into an inflamed lymph node. J Immunol 184, 2116–2123. [PubMed: 20083654]

Deckers J, Sichien D, Plantinga M, Van Moorleghem J, Vanheerswynghels M, Hoste E, Malissen B, Dombrowicz D, Guilliams M, De Bosscher K, et al. (2017). Epicutaneous sensitization to house dust mite allergen requires interferon regulatory factor 4-dependent dermal dendritic cells. J Allergy Clin Immunol 140, 1364–1377 e1362. [PubMed: 28189772]

Gao Y, Nish SA, Jiang R, Hou L, Licona-Limon P, Weinstein JS, Zhao H, and Medzhitov R (2013). Control of T helper 2 responses by transcription factor IRF4-dependent dendritic cells. Immunity 39, 722–732. [PubMed: 24076050]

Green DP, Limjunyawong N, Gour N, Pundir P, and Dong X (2019). A Mast-Cell-Specific Receptor Mediates Neurogenic Inflammation and Pain. Neuron 101, 412–420 e413. [PubMed: 30686732]

Guzman M, Miglio MS, Zgajnar NR, Colado A, Almejun MB, Keitelman IA, Sabbione F, Fuentes F, Trevani AS, Giordano MN, et al. (2018). The mucosal surfaces of both eyes are immunologically linked by a neurogenic inflammatory reflex involving TRPV1 and substance P. Mucosal Immunol 11, 1441–1453. [PubMed: 29867077]

Halim TY, Steer CA, Matha L, Gold MJ, Martinez-Gonzalez I, McNagny KM, McKenzie AN, and Takei F (2014). Group 2 innate lymphoid cells are critical for the initiation of adaptive T helper 2 cell-mediated allergic lung inflammation. Immunity 40, 425–435. [PubMed: 24613091]

Halim TYF, Rana BMJ, Walker JA, Kerscher B, Knolle MD, Jolin HE, Serrao EM, Haim-Vilmovsky L, Teichmann SA, Rodewald HR, et al. (2018). Tissue-Restricted Adaptive Type 2 Immunity Is Orchestrated by Expression of the Costimulatory Molecule OX40L on Group 2 Innate Lymphoid Cells. Immunity 48, 1195–1207 e1196. [PubMed: 29907525]

Hauser MA, Schaeuble K, Kindinger I, Impellizzieri D, Krueger WA, Hauck CR, Boyman O, and Legler DF (2016). Inflammation-Induced CCR7 Oligomers Form Scaffolds to Integrate Distinct Signaling Pathways for Efficient Cell Migration. Immunity 44, 59–72. [PubMed: 26789922]

Heng TS, Painter MW, and Immunological Genome Project C (2008). The Immunological Genome Project: networks of gene expression in immune cells. Nature immunology 9, 1091–1094. [PubMed: 18800157]

Hirata T, Morii E, Morimoto M, Kasugai T, Tsujimura T, Hirota S, Kanakura Y, Nomura S, and Kitamura Y (1993). Stem cell factor induces outgrowth of c-kit-positive neurites and supports the survival of c-kit-positive neurons in dorsal root ganglia of mouse embryos. Development 119, 49–56. [PubMed: 7506140]

Hosoi J, Murphy GF, Egan CL, Lerner EA, Grabbe S, Asahina A, and Granstein RD (1993). Regulation of Langerhans cell function by nerves containing calcitonin gene-related peptide. Nature 363, 159–163. [PubMed: 8483499]

Iida H, Takai T, Hirasawa Y, Kamijo S, Shimura S, Ochi H, Nishioka I, Maruyama N, Ogawa H, Okumura K, et al. (2014). Epicutaneous administration of papain induces IgE and IgG responses in a cysteine protease activity-dependent manner. Allergol Int 63, 219–226. [PubMed: 24662805]

Iwasaki A, and Medzhitov R (2015). Control of adaptive immunity by the innate immune system. Nature immunology 16, 343–353. [PubMed: 25789684]

Janelsins BM, Mathers AR, Tkacheva OA, Erdos G, Shufesky WJ, Morelli AE, and Larregina AT (2009). Proinflammatory tachykinins that signal through the neurokinin 1 receptor promote survival of dendritic cells and potent cellular immunity. Blood 113, 3017–3026. [PubMed: 18987361]

Janelsins BM, Sumpter TL, Tkacheva OA, Rojas-Canales DM, Erdos G, Mathers AR, Shufesky WJ, Storkus WJ, Falo LD Jr., Morelli AE, et al. (2013). Neurokinin-1 receptor agonists bias therapeutic

dendritic cells to induce type 1 immunity by licensing host dendritic cells to produce IL-12. Blood 121, 2923–2933. [PubMed: 23365459]

Joost S, Annusver K, Jacob T, Sun X, Dalessandri T, Sivan U, Sequeira I, Sandberg R, and Kasper M (2020). The Molecular Anatomy of Mouse Skin during Hair Growth and Rest. Cell Stem Cell 26, 441–457 e447. [PubMed: 32109378]

Kashem SW, Riedl MS, Yao C, Honda CN, Vulchanova L, and Kaplan DH (2015). Nociceptive Sensory Fibers Drive Interleukin-23 Production from CD301b+ Dermal Dendritic Cells and Drive Protective Cutaneous Immunity. Immunity 43, 515–526. [PubMed: 26377898]

Kumamoto Y, Linehan M, Weinstein JS, Laidlaw BJ, Craft JE, and Iwasaki A (2013). CD301b(+) dermal dendritic cells drive T helper 2 cell-mediated immunity. Immunity 39, 733–743. [PubMed: 24076051]

Lai NY, Musser MA, Pinho-Ribeiro FA, Baral P, Jacobson A, Ma P, Potts DE, Chen Z, Paik D, Soualhi S, et al. (2019). Gut-Innervating Nociceptor Neurons Regulate Peyer's Patch Microfold Cells and SFB Levels to Mediate Salmonella Host Defense. Cell.

Lamhamedi-Cherradi SE, Martin RE, Ito T, Kheradmand F, Corry DB, Liu YJ, and Moyle M (2008). Fungal proteases induce Th2 polarization through limited dendritic cell maturation and reduced production of IL-12. J Immunol 180, 6000–6009. [PubMed: 18424720]

Lin YP, Nelson C, Kramer H, and Parekh AB (2018). The Allergen Der p3 from House Dust Mite Stimulates Store-Operated Ca(2+) Channels and Mast Cell Migration through PAR4 Receptors. Mol Cell 70, 228–241 e225. [PubMed: 29677491]

Liu Q, Tang Z, Surdenikova L, Kim S, Patel KN, Kim A, Ru F, Guan Y, Weng HJ, Geng Y, et al. (2009). Sensory neuron-specific GPCR Mrgprs are itch receptors mediating chloroquine-induced pruritus. Cell 139, 1353–1365. [PubMed: 20004959]

Liu Q, Weng HJ, Patel KN, Tang Z, Bai H, Steinhoff M, and Dong X (2011). The distinct roles of two GPCRs, MrgprC11 and PAR2, in itch and hyperalgesia. Sci Signal 4, ra45. [PubMed: 21775281]

Liu YJ, Soumelis V, Watanabe N, Ito T, Wang YH, Malefyt Rde W, Omori M, Zhou B, and Ziegler SF (2007). TSLP: an epithelial cell cytokine that regulates T cell differentiation by conditioning dendritic cell maturation. Annu Rev Immunol 25, 193–219. [PubMed: 17129180]

Mathers AR, Tckacheva OA, Janelsins BM, Shufesky WJ, Morelli AE, and Larregina AT (2007). In vivo signaling through the neurokinin 1 receptor favors transgene expression by Langerhans cells and promotes the generation of Th1- and Tc1-biased immune responses. J Immunol 178, 7006–7017. [PubMed: 17513750]

Mazzoni A, Siraganian RP, Leifer CA, and Segal DM (2006). Dendritic cell modulation by mast cells controls the Th1/Th2 balance in responding T cells. J Immunol 177, 3577–3581. [PubMed: 16951316]

McNeil BD, Pundir P, Meeker S, Han L, Undem BJ, Kulka M, and Dong X (2015). Identification of a mast-cell-specific receptor crucial for pseudo-allergic drug reactions. Nature 519, 237–241. [PubMed: 25517090]

Meixiong J, Anderson M, Limjunyawong N, Sabbagh MF, Hu E, Mack MR, Oetjen LK, Wang F, Kim BS, and Dong X (2019a). Activation of Mast-Cell-Expressed Mas-Related G-Protein-Coupled Receptors Drives Non-histaminergic Itch. Immunity 50, 1163–1171 e1165. [PubMed: 31027996]

Meixiong J, Vasavda C, Green D, Zheng Q, Qi L, Kwatra SG, Hamilton JP, Snyder SH, and Dong X (2019b). Identification of a bilirubin receptor that may mediate a component of cholestatic itch. Elife 8.

Migueres M, Davila I, Frati F, Azpeitia A, Jeanpetit Y, Lheritier-Barrand M, Incorvaia C, and Ciprandi G (2014). Types of sensitization to aeroallergens: definitions, prevalences and impact on the diagnosis and treatment of allergic respiratory disease. Clin Transl Allergy 4, 16. [PubMed: 24817997]

Milenkovic N, Frahm C, Gassmann M, Griffel C, Erdmann B, Birchmeier C, Lewin GR, and Garratt AN (2007). Nociceptive tuning by stem cell factor/c-Kit signaling. Neuron 56, 893–906. [PubMed: 18054864]

Mohrs M, Shinkai K, Mohrs K, and Locksley RM (2001). Analysis of type 2 immunity in vivo with a bicistronic IL-4 reporter. Immunity 15, 303–311. [PubMed: 11520464]

Oetjen LK, Mack MR, Feng J, Whelan TM, Niu H, Guo CJ, Chen S, Trier AM, Xu AZ, Tripathi SV, et al. (2017). Sensory Neurons Co-opt Classical Immune Signaling Pathways to Mediate Chronic Itch. Cell 171, 217–228 e213. [PubMed: 28890086]

Ohl L, Mohaupt M, Czeloth N, Hintzen G, Kiafard Z, Zwirner J, Blankenstein T, Henning G, and Forster R (2004). CCR7 governs skin dendritic cell migration under inflammatory and steady-state conditions. Immunity 21, 279–288. [PubMed: 15308107]

Palm NW, Rosenstein RK, and Medzhitov R (2012). Allergic host defences. Nature 484, 465–472. [PubMed: 22538607]

Palm NW, Rosenstein RK, Yu S, Schenten DD, Florsheim E, and Medzhitov R (2013). Bee venom phospholipase A2 induces a primary type 2 response that is dependent on the receptor ST2 and confers protective immunity. Immunity 39, 976–985. [PubMed: 24210353]

Pinho-Ribeiro FA, Baddal B, Haarsma R, O'Seaghdha M, Yang NJ, Blake KJ, Portley M, Verri WA, Dale JB, Wessels MR, et al. (2018). Blocking Neuronal Signaling to Immune Cells Treats Streptococcal Invasive Infection. Cell 173, 1083–1097 e1022. [PubMed: 29754819]

Pogorzala LA, Mishra SK, and Hoon MA (2013). The cellular code for mammalian thermosensation. J Neurosci 33, 5533–5541. [PubMed: 23536068]

Porter P, Susarla SC, Polikepahad S, Qian Y, Hampton J, Kiss A, Vaidya S, Sur S, Ongeri V, Yang T, et al. (2009). Link between allergic asthma and airway mucosal infection suggested by proteinase-secreting household fungi. Mucosal Immunol 2, 504–517. [PubMed: 19710638]

Rank MA, Kobayashi T, Kozaki H, Bartemes KR, Squillace DL, and Kita H (2009). IL-33-activated dendritic cells induce an atypical TH2-type response. J Allergy Clin Immunol 123, 1047–1054. [PubMed: 19361843]

Reddy VB, and Lerner EA (2010). Plant cysteine proteases that evoke itch activate protease-activated receptors. Br J Dermatol 163, 532–535. [PubMed: 20491769]

Reddy VB, Sun S, Azimi E, Elmariah SB, Dong X, and Lerner EA (2015). Redefining the concept of protease-activated receptors: cathepsin S evokes itch via activation of Mrgprs. Nat Commun 6, 7864. [PubMed: 26216096]

Riol-Blanco L, Ordovas-Montanes J, Perro M, Naval E, Thiriot A, Alvarez D, Paust S, Wood JN, and von Andrian UH (2014). Nociceptive sensory neurons drive interleukin-23-mediated psoriasiform skin inflammation. Nature 510, 157–161. [PubMed: 24759321]

Roberson DP, Gudes S, Sprague JM, Patoski HA, Robson VK, Blasl F, Duan B, Oh SB, Bean BP, Ma Q, et al. (2013). Activity-dependent silencing reveals functionally distinct itch-generating sensory neurons. Nat Neurosci 16, 910–918. [PubMed: 23685721]

Serhan N, Basso L, Sibilano R, Petitfils C, Meixiong J, Bonnart C, Reber LL, Marichal T, Starkl P, Cenac N, et al. (2019). House dust mites activate nociceptor-mast cell clusters to drive type 2 skin inflammation. Nature immunology 20, 1435–1443. [PubMed: 31591569]

Shelburne CP, Nakano H, St John AL, Chan C, McLachlan JB, Gunn MD, Staats HF, and Abraham SN (2009). Mast cells augment adaptive immunity by orchestrating dendritic cell trafficking through infected tissues. Cell Host Microbe 6, 331–342. [PubMed: 19837373]

Sokol CL, Barton GM, Farr AG, and Medzhitov R (2008). A mechanism for the initiation of allergen-induced T helper type 2 responses. Nature immunology 9, 310–318. [PubMed: 18300366]

Sokol CL, Camire RB, Jones MC, and Luster AD (2018). The Chemokine Receptor CCR8 Promotes the Migration of Dendritic Cells into the Lymph Node Parenchyma to Initiate the Allergic Immune Response. Immunity 49, 449–463 e446. [PubMed: 30170811]

Stirling LC, Forlani G, Baker MD, Wood JN, Matthews EA, Dickenson AH, and Nassar MA (2005). Nociceptor-specific gene deletion using heterozygous NaV1.8-Cre recombinase mice. Pain 113, 27–36. [PubMed: 15621361]

Strid J, Hourihane J, Kimber I, Callard R, and Strobel S (2004). Disruption of the stratum corneum allows potent epicutaneous immunization with protein antigens resulting in a dominant systemic Th2 response. Eur J Immunol 34, 2100–2109. [PubMed: 15259007]

Takagi K, Okuda-Ashitaka E, Mabuchi T, Katano T, Ohnishi T, Matsumura S, Ohnaka M, Kaneko S, Abe T, Hirata T, et al. (2008). Involvement of stem cell factor and its receptor tyrosine kinase c-kit in pain regulation. Neuroscience 153, 1278–1288. [PubMed: 18423881]

Talbot S, Abdulnour RE, Burkett PR, Lee S, Cronin SJ, Pascal MA, Laedermann C, Foster SL, Tran JV, Lai N, et al. (2015). Silencing Nociceptor Neurons Reduces Allergic Airway Inflammation. Neuron 87, 341–354. [PubMed: 26119026]

Talbot S, Foster SL, and Woolf CJ (2016). Neuroimmunity: Physiology and Pathology. Annu Rev Immunol 34, 421–447. [PubMed: 26907213]

Tang H, Cao W, Kasturi SP, Ravindran R, Nakaya HI, Kundu K, Murthy N, Kepler TB, Malissen B, and Pulendran B (2010). The T helper type 2 response to cysteine proteases requires dendritic cell-basophil cooperation via ROS-mediated signaling. Nature immunology 11, 608–617. [PubMed: 20495560]

Tomura M, Yoshida N, Tanaka J, Karasawa S, Miwa Y, Miyawaki A, and Kanagawa O (2008). Monitoring cellular movement in vivo with photoconvertible fluorescence protein "Kaede" transgenic mice. Proc Natl Acad Sci U S A 105, 10871–10876. [PubMed: 18663225]

Trankner D, Hahne N, Sugino K, Hoon MA, and Zuker C (2014). Population of sensory neurons essential for asthmatic hyperreactivity of inflamed airways. Proc Natl Acad Sci U S A 111, 11515–11520. [PubMed: 25049382]

Trier AM, Mack MR, and Kim BS (2019). The Neuroimmune Axis in Skin Sensation, Inflammation, and Immunity. J Immunol 202, 2829–2835. [PubMed: 31061146]

Tussiwand R, Everts B, Grajales-Reyes GE, Kretzer NM, Iwata A, Bagaitkar J, Wu X, Wong R, Anderson DA, Murphy TL, et al. (2015). Klf4 expression in conventional dendritic cells is required for T helper 2 cell responses. Immunity 42, 916–928. [PubMed: 25992862]

Usoskin D, Furlan A, Islam S, Abdo H, Lonnerberg P, Lou D, Hjerling-Leffler J, Haeggstrom J, Kharchenko O, Kharchenko PV, et al. (2015). Unbiased classification of sensory neuron types by large-scale single-cell RNA sequencing. Nat Neurosci 18, 145–153. [PubMed: 25420068]

Van Dyken SJ, and Locksley RM (2018). Chitins and chitinase activity in airway diseases. J Allergy Clin Immunol 142, 364–369. [PubMed: 29959948]

Veiga-Fernandes H, and Mucida D (2016). Neuro-Immune Interactions at Barrier Surfaces. Cell 165, 801–811. [PubMed: 27153494]

Xu J, Zanvit P, Hu L, Tseng PY, Liu N, Wang F, Liu O, Zhang D, Jin W, Guo N, et al. (2020). The Cytokine TGF-beta Induces Interleukin-31 Expression from Dermal Dendritic Cells to Activate Sensory Neurons and Stimulate Wound Itching. Immunity.

Yosipovitch G, Stander S, Kerby MB, Larrick JW, Perlman AJ, Schnipper EF, Zhang X, Tang JY, Luger T, and Steinhoff M (2018). Serlopitant for the treatment of chronic pruritus: Results of a randomized, multicenter, placebo-controlled phase 2 clinical trial. J Am Acad Dermatol 78, 882–891 e810. [PubMed: 29462657]

Zylka MJ, Rice FL, and Anderson DJ (2005). Topographically distinct epidermal nociceptive circuits revealed by axonal tracers targeted to Mrgprd. Neuron 45, 17–25. [PubMed: 15629699]

HIGHLIGHTS

- Allergens activate sensory neurons to induce itch responses and Substance P release
- Allergen-activated TRPV1$^+$ neurons trigger CD301b$^+$ DC migration to the lymph node
- Substance P directly induces CD301b$^+$ DC migration through MRGPRA1
- TRPV1$^+$ neurons are required for Th2-differentiation in response to allergens

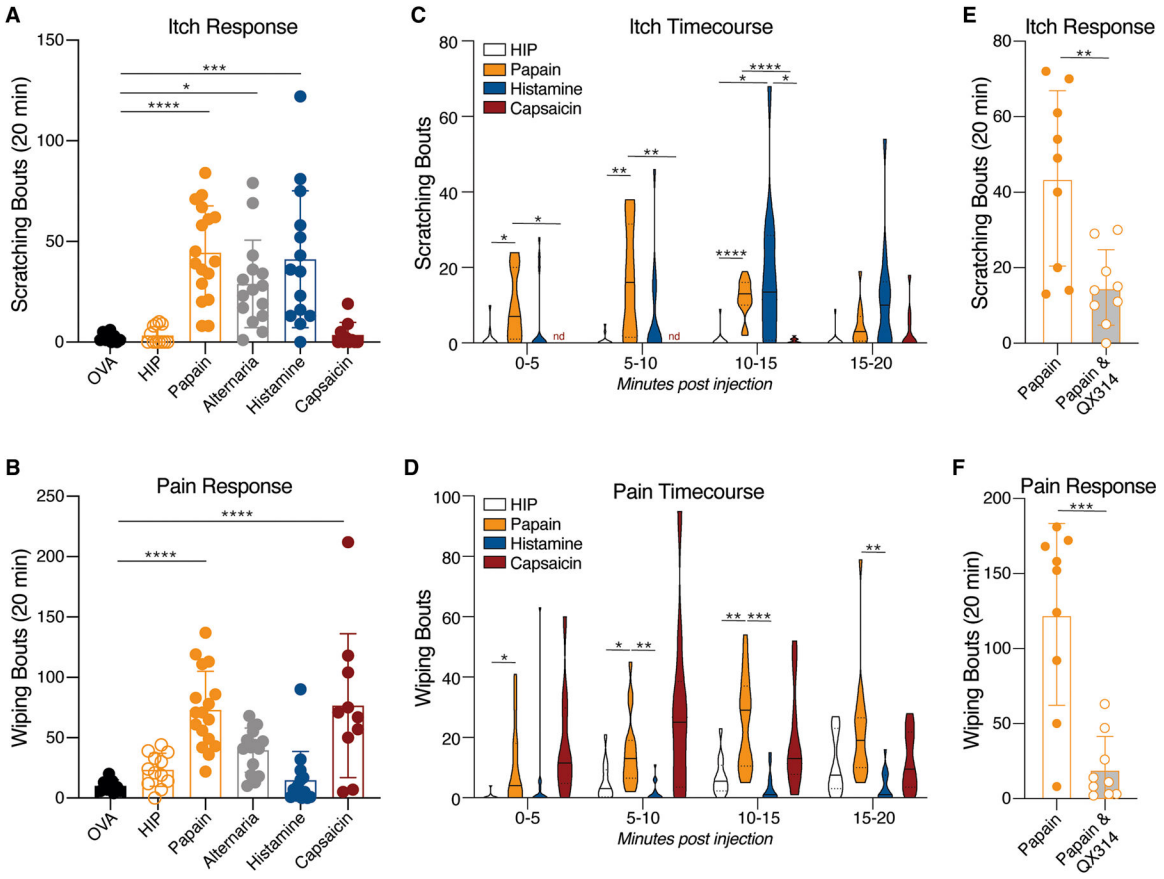

Figure 1. The protease allergen papain induces an immediate sensory response.

(**A** and **B**) Wild type (WT) mice were intradermally (i.d.) injected with ovalbumin (OVA), heat inactivated papain (HIP), papain, Alternaria extract, histamine, or capsaicin. The total number of ipsilateral cheek (A) scratch events or (B) wipe events. (**C** and **D**) Timecourse of (C) scratch or (D) wipe events in 5 minute increments. (**E** and **F**) Total scratch (E) and wipe (F) events after indicated i.d. injection. Symbols represent individual mice (A, B, E, F), bars indicate mean, and error bars indicate SEM. Violin plots (C and D) show grouped timecourse data from (A and B); line indicates median, dotted lines indicate quartiles, and nd indicates not detected. Statistical tests: Ordinary one-way ANOVA with multiple comparisons (A and B), two-way ANOVA with multiple comparisons (C and D), and unpaired t test (E and F). * $p<0.05$, ** $p<0.01$, *** $p<0.001$, **** $p<0.0001$. Data are representative of at least three independent experiments combined with each experiment including 3–5 mice per group.

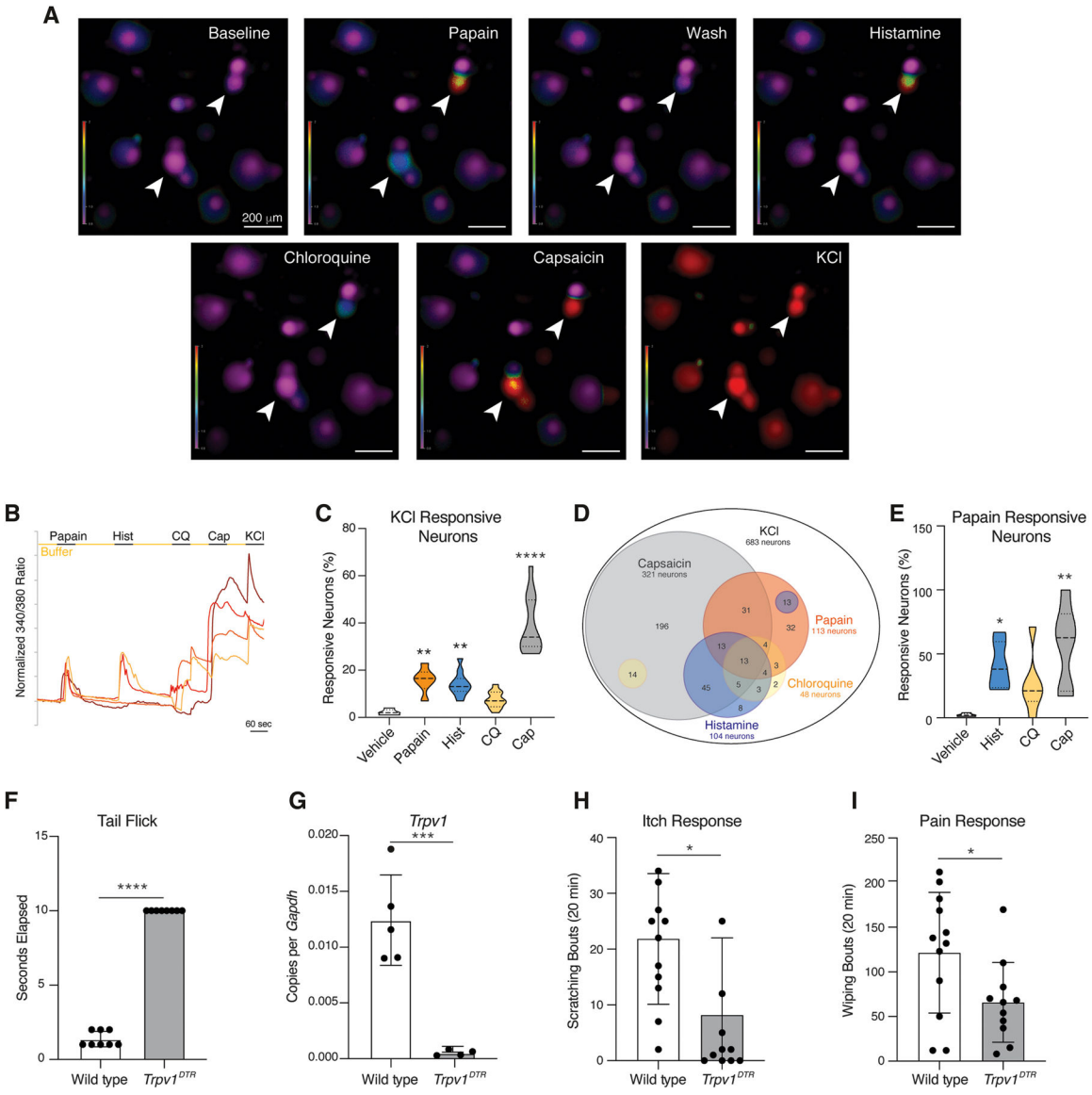

Figure 2. TRPV1^{+} neurons are directly activated by papain and are required for the papain-induced sensory response.

(**A**) Representative Fura-2-AM ratiometric fields of cultured DRG neurons at baseline and after sequential treatment as shown with wash steps in between all stimuli. (**B**) Calcium (Ca^{2+}) traces of representative DRG neurons (colored separately for identification) treated as in (A). (**C**) The percent of total excitable (KCl responsive) DRG neurons that responded to the indicated treatments. (**D**) Venn diagram showing responsiveness of individual DRG neurons. (**E**) The percent of papain responsive DRG neurons that also responded to the indicated stimuli as compared to the total vehicle responsive neurons. (C-E) Data were calculated from 12 fields of view and 1389 neurons that were sequentially stimulated with papain (6 fields of view and 705 neurons) or vehicle (6 fields of view and 684 neurons) followed by histamine, chloroquine, capsaicin and KCl. (**F**) Tail flick assay of WT or *Trpv1*^{DTR} mice intraperitoneally injected with DT. (**G**) QPCR analysis of *Trpv1* from DRG of DT treated WT or *Trpv1*^{DTR} mice. (**H** and **I**) Total scratching (H) or wiping (I) events in

DT treated WT or *Trpv1*^{DTR} mice after papain injection. Symbols represent individual mice (F, G, H, I), bar indicates mean, and error bars indicate SEM. Violin plot (C and E) lines indicate median, dotted lines indicate quartiles. Statistical tests: Ordinary on-way ANOVA with multiple comparisons (C and E), unpaired t test (F, G, H, I). * $p<0.05$, ** $p<0.01$, *** $p<0.001$, **** $p<0.0001$. Data are representative of at least three independent experiments combined with each experiment including 3–5 mice per group.

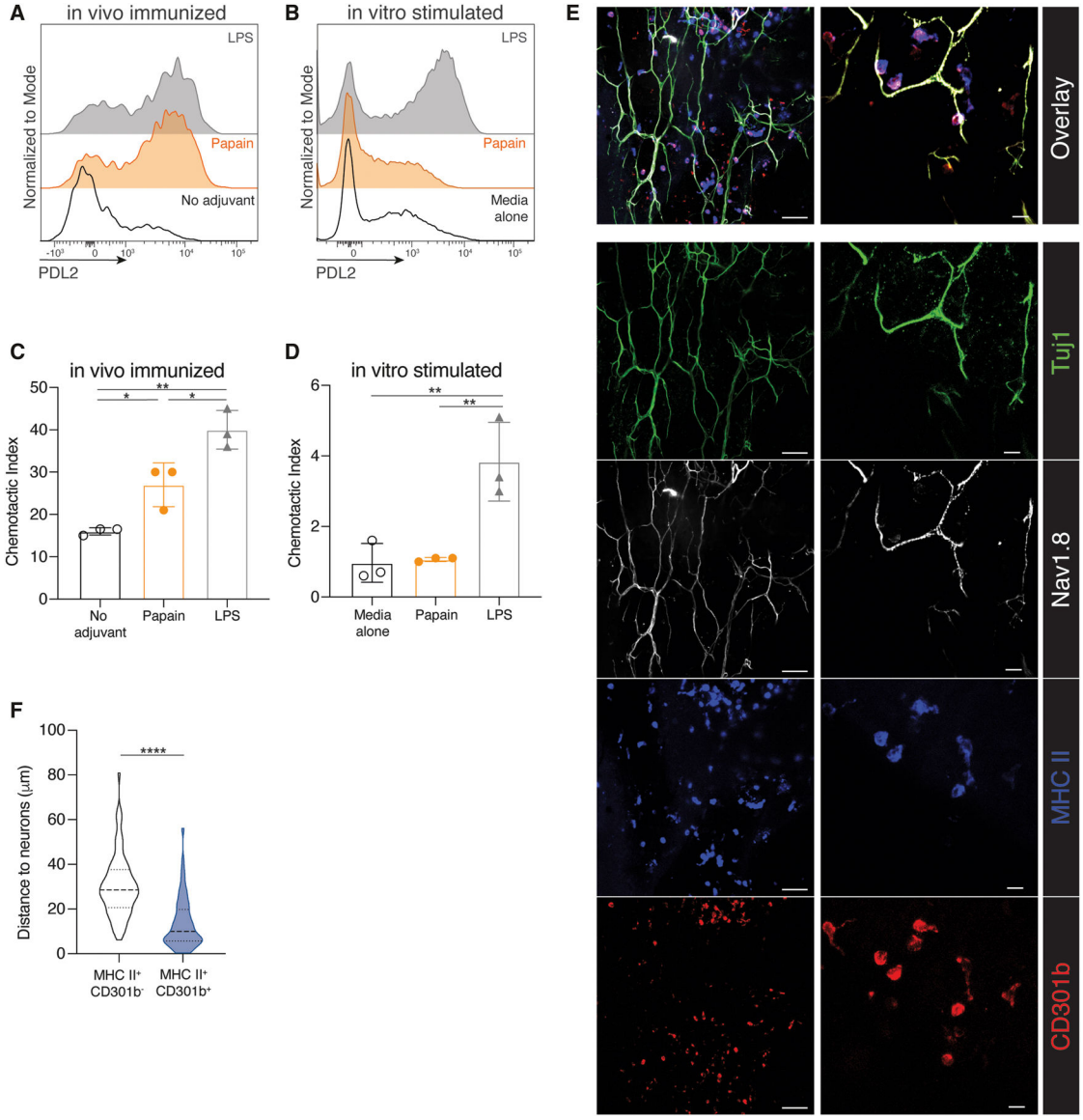

Figure 3. CD301b$^+$ dendritic cells do not respond directly to the protease allergen papain and are found in close proximity to sensory neurons in the dermis.

(**A**) Flow cytometry of PDL2 expression on live CD11c$^+$CD301b$^+$ DCs from the dLN 24 hours after i.d. immunization with OVA (No adjuvant), OVA and papain (Papain), or OVA and LPS. (**B**) Flow cytometry of PDL2 expression on live CD11c$^+$CD301b$^+$ BMDCs after overnight stimulation with media, papain, or LPS. (**C** and **D**) Transwell migration to CCL21, normalized to media only control (chemotactic index), of (C) CD11c$^+$CD301b$^+$ cells sorted from the dLN of mice immunized as in (A), or of (D) BMDCs stimulated as in (B). (**E**) Confocal immunofluorescence microscopy of naïve dermal sheets from *Nav1.8^{tdTomato}* (white) mice stained with Tuj1 (green), MHCII (blue) and CD301b (red). Scale bar in left 20x panels shows 50 µm, scale bar in right 63x panels shows 10 µm. (**F**) Closest distance (µm) between MHCII$^+$CD301b$^-$ (white, N=81) and MHCII$^+$CD301b$^+$ (blue, N=122) cells and tdTomato$^+$ neurons from naïve *Nav1.8^{tdTomato}* mice (10 fields of view). Symbols represent individual replicates (C and D). Bars indicate mean and error bars indicate SEM.

Solid lines on violin plots (F) indicate median, dotted lines indicate quartiles. Statistical tests: Ordinary one-way ANOVA with multiple comparisons (C and D), unpaired t test (F). * $p<0.05$, ** $p<0.01$, *** $p<0.001$, **** $p<0.0001$. Data are representative of at least three experiments (A–F), combined in F with each experiment including 2–5 mice per group. Please also see Figure S1.

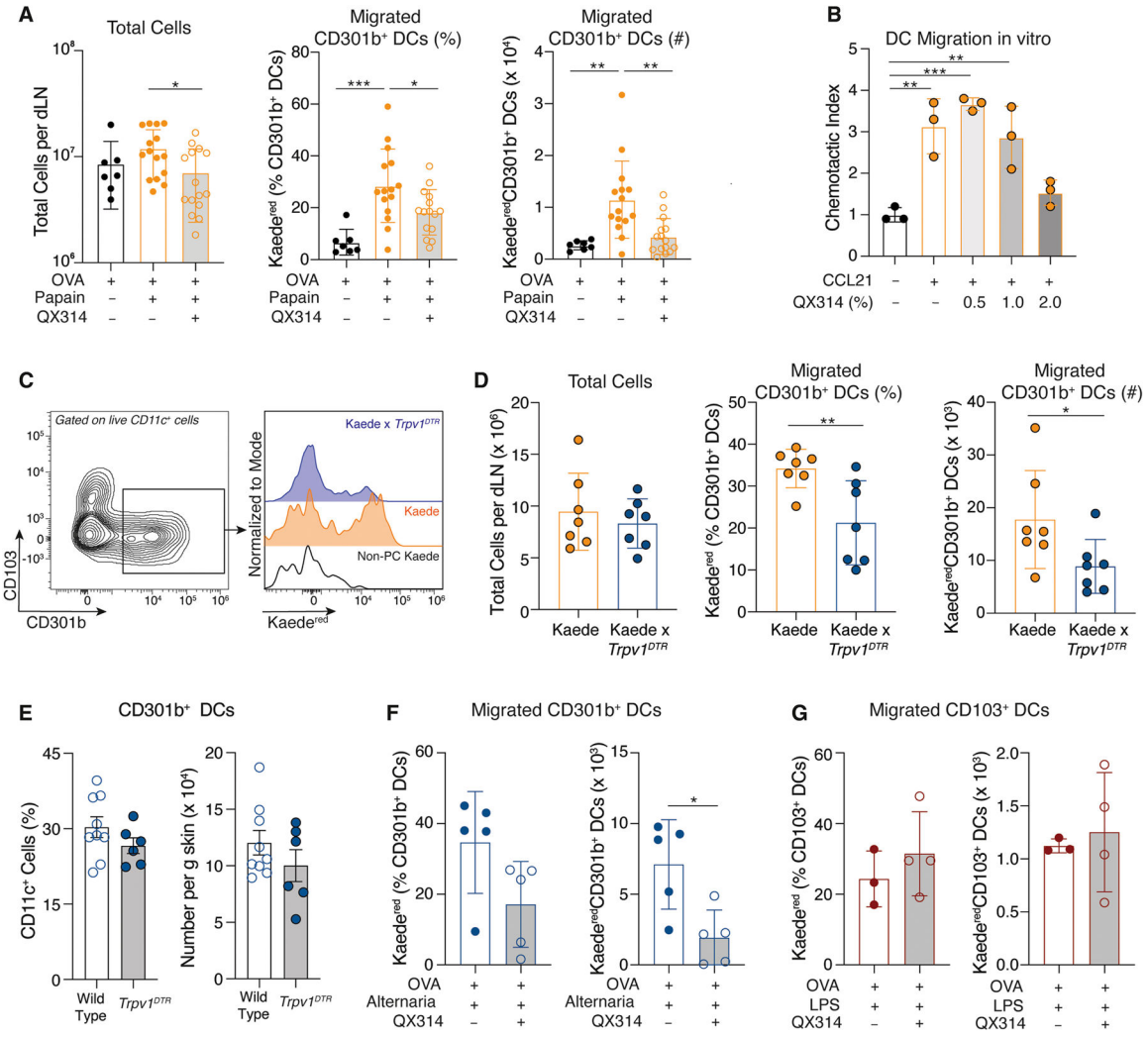

Figure 4. Allergen-induced migration of cutaneous Th2 cell skewing CD301b$^+$ dendritic cells into the draining lymph node requires TRPV1$^+$ sensory neurons.

(**A**) Total cells per dLN, and percent and number of CD11c$^+$CD301b$^+$ cells (CD301b$^+$ DCs) that migrated from the skin of photoconverted (PC) Kaede transgenic mice (Kaede^{red}) to the dLN 24 hours post i.d. injection as indicated. (**B**) Transwell migration of BMDCs stimulated overnight with LPS to CCL21 in the presence of 0.5%, 1%, and 2% QX314. (**C**) Flow cytometry of CD301b$^+$ DCs from the dLN of DT treated Kaede or Kaede x *Trpv1^{DTR}* mice 24 hours after PC and i.d. immunization with papain. (**D**) Total cells per dLN, and percent and number of Kaede^{red}CD301b$^+$ DCs was quantified by flow cytometry from mice treated as in (C). (**E**) Percent or number per gram (g) skin of CD45$^+$CD11c$^+$MHCII$^+$CD301b$^+$ DCs in DT treated WT or *Trpv1^{DTR}* mice. (**F and G**) Photoconverted Kaede mice were immunized with (F) OVA and Alternaria extract or (G) OVA and LPS in the presence or absence of 1% QX314. The percent and total number of Kaede^{red} (F) CD301b$^+$ DCs or (G) CD103$^+$ DCs, were quantified by flow cytometry. Symbols represent individual mice (A, D–G) or replicates (B). Bars indicate mean and error bars indicate SEM. Statistical tests: Ordinary one-way ANOVA with multiple comparisons (A and B), unpaired t test (D-G). * p<0.05, ** p<0.01, *** p<0.001, **** p<0.0001. Data are representative of at least three

(A–D) or two (E–G) independent experiments, combined in A, D, and E with each experiment including 2–5 (A and D) or 5–9 (E) mice per group. Please also see Figure S2.

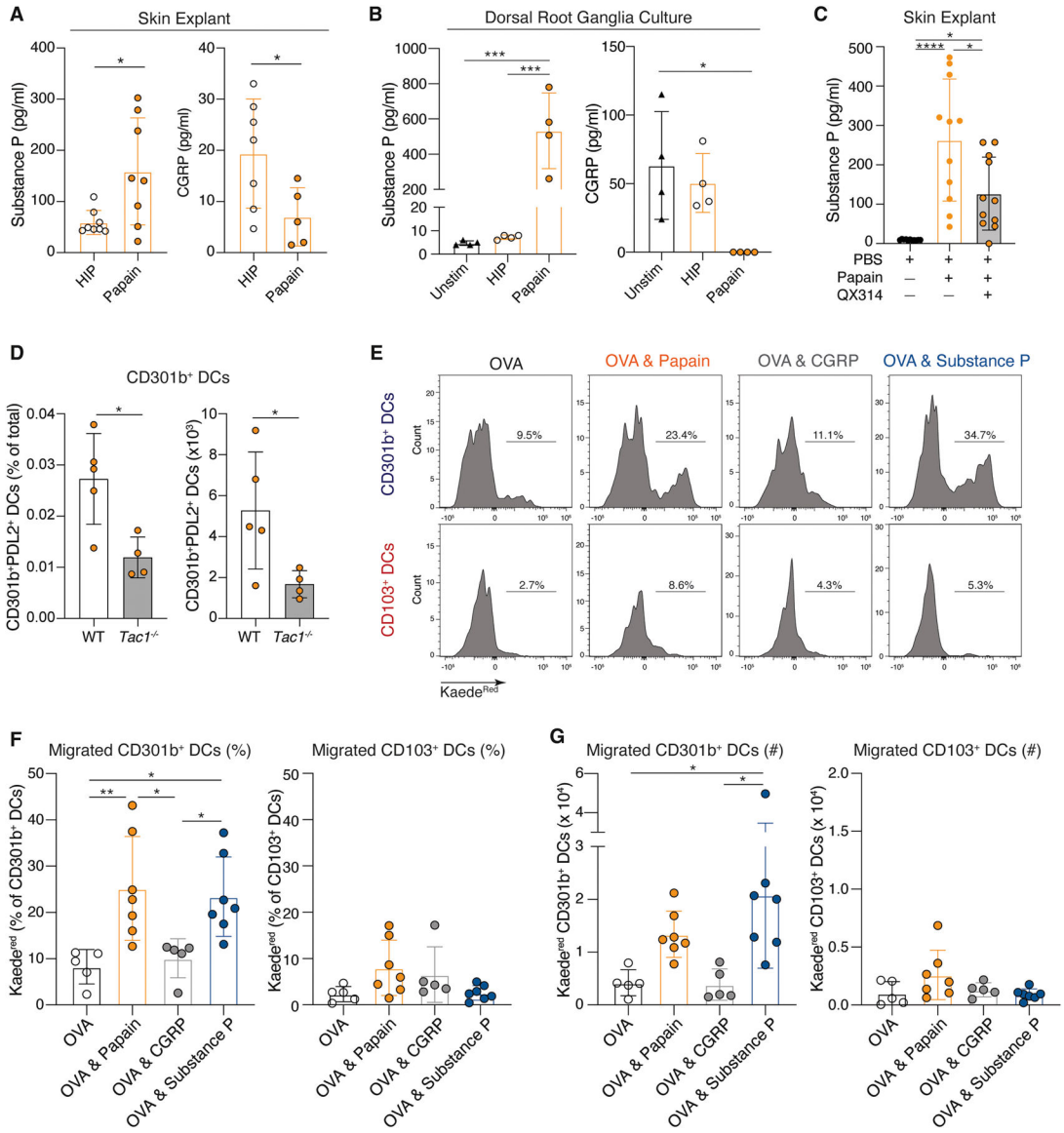

Figure 5. Allergen-stimulated sensory neurons release Substance P, which induces the specific migration of Th2 cell-skewing CD301b$^+$ dendritic cells into the draining lymph node.

(**A**) ELISA for SP and CGRP of skin explant supernatants from WT mice i.d. injected as indicated. (**B**) Cultured WT DRG were stimulated as indicated and supernatant was assayed as in (A). (**C**) SP release from skin explants of WT mice i.d. injected as indicated. (**D**) Percent and number of PDL2$^+$CD301b$^+$ DCs per dLN of WT or *Tac1*$^{-/-}$ mice 24 hours after i.d. immunization with OVA & papain. (**E-G**) Flow cytometry of Kaede^{red} live CD11c$^+$CD301b$^+$ DCs or CD11c$^+$CD103$^+$ DCs 24 hours after photoconversion and the indicated immunization, shown as histograms (E), percent (F), or total number (G). Symbols represent individual mice (A, C, D, F, G) or replicates (B). Bars indicate mean and error bars indicate SEM. Statistical tests: unpaired t test (A, D), ordinary one-way ANOVA with multiple comparisons (B, C, F, G). * $p<0.05$, ** $p<0.01$, *** $p<0.001$. Data are representative of at least three independent experiments (B, D), combined in (A, C, F, G), with each experiment including 2–4 mice per group. Please also see Figures S3–S5.

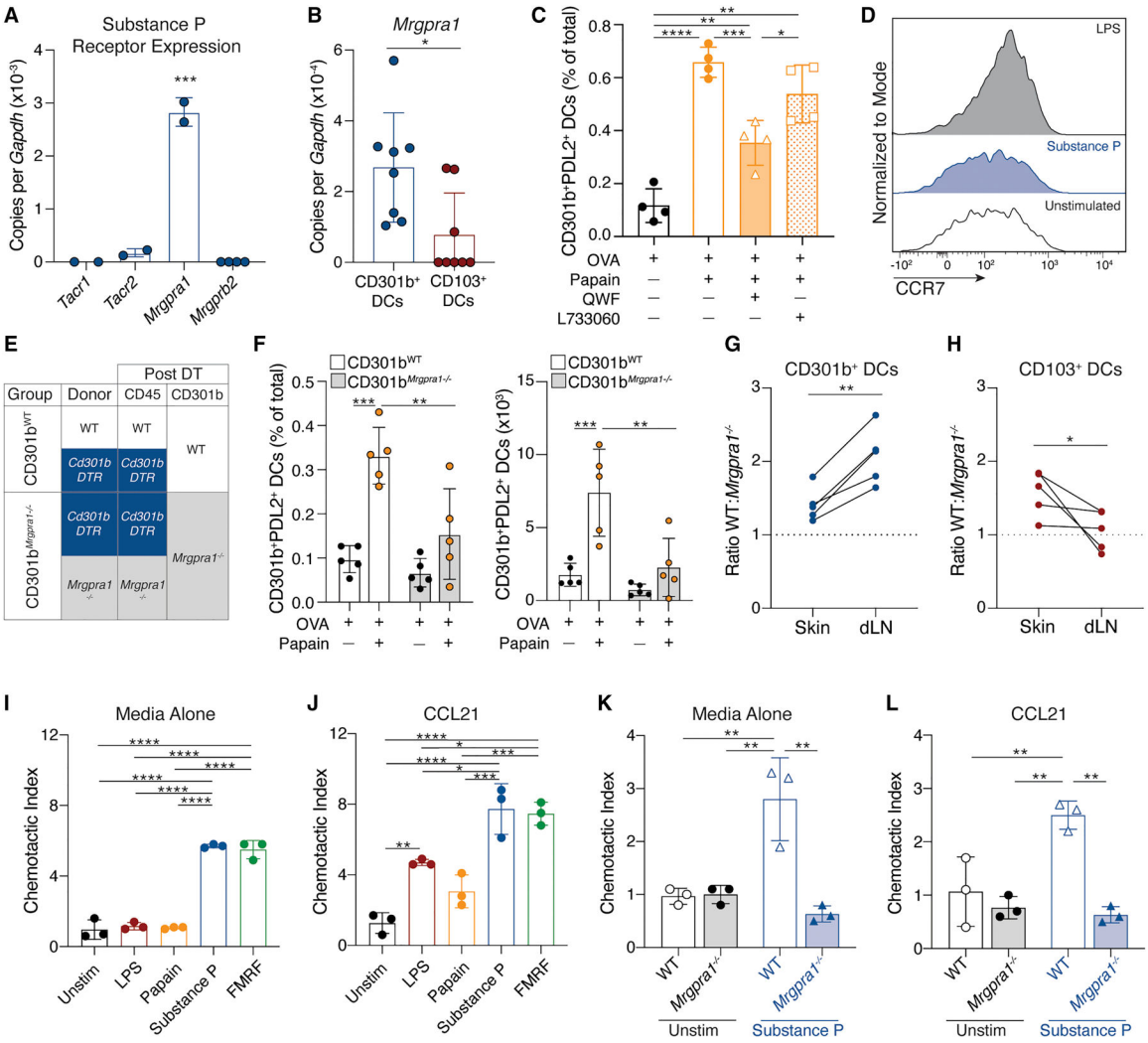

Figure 6. Substance P promotes Th2 cell-skewing CD301b$^+$ dendritic cell migration through its receptor *Mrgpra1*.

(**A**) QPCR analysis of *Tacr1*, *Tacr2*, *Mrgpra1* and *Mrgprb2* from unstimulated BMDCs. (**B**) QPCR analysis of *Mrpgra1* expression on live CD11c$^+$CD301b$^+$ (CD301b$^+$ DCs) or CD11c$^+$CD103$^+$ (CD103$^+$ DCs) cells flow sorted from the dLN of wild type mice immunized i.d. with papain. (**C**) CD301b$^+$PDL2$^+$ DCs in the dLN 24 hours after the indicated immunizations. (**D**) CCR7 expression by flow cytometry of unstimulated (white), SP stimulated (blue), or LPS stimulated (black) CD11c$^+$CD301b$^+$. (**E**) Generation of BM chimeras for comparative migration. (**F**) BM chimeras in (E) were treated with DT, immunized as indicated, and the percentage and absolute number of PDL2$^+$ CD301b$^+$ DCs in dLNs were calculated. (**G-H**) Mixed BM chimeras of equal ratios of CD45.1$^+$ wild type and CD45.2$^+$ *Mrgpra1*$^{-/-}$BM into lethally irradiated wild type recipients were generated. Ratios of wild type over *Mrgpra1*$^{-/-}$ (G) CD11c$^+$CD301b$^+$ or (H) CD11c$^+$CD103$^+$ cells from naïve ear skin and the dLN 24 hours after i.d. (G) papain or (H) LPS immunization of the footpad. Data normalized to total CD45$^+$ cells. (**I–J**) Wild type BMDCs were stimulated overnight as indicated. Transwell migration to media alone (I) or CCL21 (J), normalized to unstimulated BMDCs (chemotactic index). (**K–L**) Transwell migration of unstimulated or

SP stimulated wild type or *Mrgra1*$^{-/-}$ BMDCs as in (I–J). Symbols represent individual replicates (A, B,I–L) or mice (C, F–H), with each mouse serving as its own control in F–H. Histograms are representative individual samples (D). Bars indicate mean and error bars indicate SEM. Statistical tests: Ordinary one-way ANOVA with multiple comparisons (A, C, F, I–L), unpaired t test (B), paired t-test (G, H). * $p<0.05$, ** $p<0.01$, *** $p<0.001$, **** $p<0.0001$. Data are representative of at least two independent experiments, combined in (B, C, H) with each experiment including 2–5 mice per group. Please also see Figure S6.

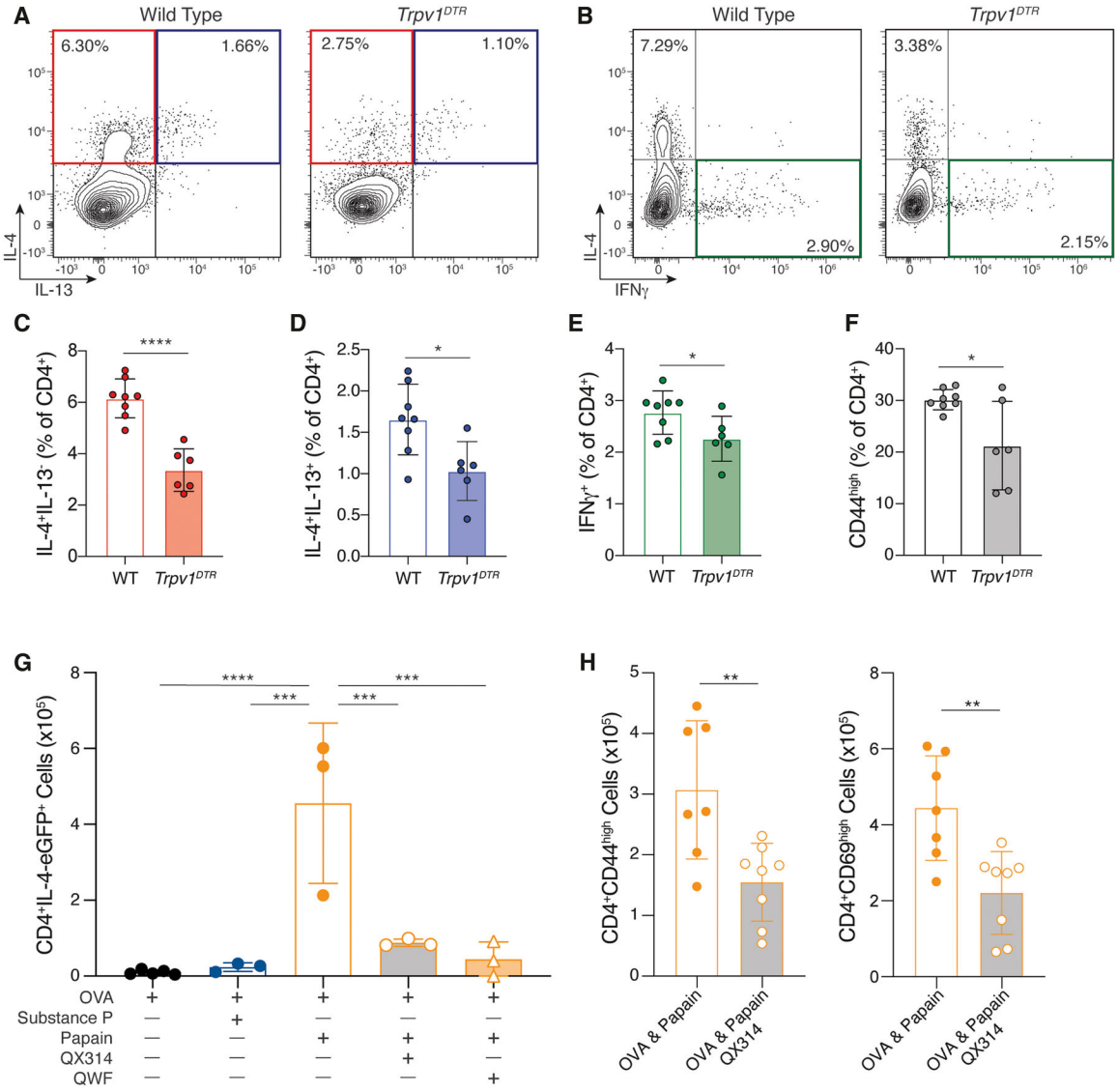

Figure 7. TRPV1$^+$ neurons are required for Th2 cell differentiation in response to the protease allergen papain.

(**A** and **B**) DT treated wild type or *Trpv1^{DTR}* mice were immunized with OVA & papain, and 5 days later flow cytometry was performed for IL-4 and IL-13 (A) or IFN**γ** (B). (**C-E**) Percent of CD4$^+$ cells gated as in A and B, or (**F**) CD44^{high}. (**G**) CD4$^+$IL-4-eGFP$^+$ cells from the dLN of 4get (*IL-4^{eGFP}*) mice 4 days after the indicated immunizations. (**H**) CD4$^+$ CD44^{high} or CD69^{high} cells in the dLN 5 days after the indicated immunization. Symbols represent individual mice (C–F). Bars indicate mean and error bars indicate SEM. Statistical tests: Ordinary one-way ANOVA with multiple comparisons (G), unpaired t test (C–F, H). * p<0.05, ** p<0.01, *** p<0.001, **** p<0.0001. Data are representative of at least two independent experiments, with each experiment including 2–5 mice per group.

Key Resources Table

Reagent/Material	Source	Identifier
Antibodies:		
Anti-mouse CD103, Clone:M290	BioLegend	Cat#: 740355
Anti-mouse CD117(c-kit), Clone: 2B8	BioLegend	Cat#: 105839
Anti-mouse CD117(c-kit), Clone: 2B8	BioLegend	Cat#: 105813
Anti-mouse CD117(c-kit), Clone: 2B8	BioLegend	Cat#: 105815
Anti-mouse CD11b, Clone: M1/70	BD Biosciences	Cat#: 553312
Anti-mouse/human CD11b, Clone: M1/70	BioLegend	Cat#: 101208
Anti-mouse CD11b, Clone: M1/70	BioLegend	Cat#: 101251
Anti-mouse CD11b, Clone: M1/70	BioLegend	Cat#: 101217
Anti-mouse CD11b, Clone: M1/70	eBioscience	Cat#: 25–0112-82
Anti-mouse CD11c, Clone: HL3	BD Biosciences	Cat#: 562782
Anti-mouse CD11c, Clone: HL3	BD Biosciences	Cat#: 553801
Anti-mouse CD11c, Clone: N418	BioLegend	Cat#: 117334
Anti-mouse CD11c, Clone: N418	BioLegend	Cat#: 117353
Anti-mouse CD273 (PDL2), Clone: TY25	BioLegend	Cat#: 107210
Anti-mouse CD3, Clone: 17A2	BioLegend	Cat#: 100204
Anti-mouse CD3ε, Clone: 145–2C11	BioLegend	Cat#: 100351
Anti-mouse CD301b (MGL2), Clone: URA-1	BioLegend	Cat#: 146808
Anti-mouse CD4, Clone: GK1.5	BioLegend	Cat#: 100437
Anti-mouse CD4, Clone: GK1.5	BioLegend	Cat#: 100451
Anti-mouse CD4, Clone: RM4–5	BioLegend	Cat#: 100516
Anti-mouse CD4, Clone: GK1.5	BioLegend	Cat#: 100408
Anti-mouse/human CD44, Clone: IM7	BioLegend	Cat#: 103025
Anti-mouse CD45, Clone: 30-F11	BioLegend	Cat#: 103124
Anti-mouse CD45, Clone: 30-F11	BioLegend	Cat#: 103151
Anti-mouse CD45.1, Clone: A20	BioLegend	Cat#: 110708
Anti-mouse CD45.2, Clone: 104	BioLegend	Cat#: 109818
Anti-mouse CD69, Clone: H1.2F3	BioLegend	Cat#: 104543
Anti-mouse CD8α, Clone: 53–6.7	BioLegend	Cat#: 100722
Anti-mouse CD86, Clone: PO3	BioLegend	Cat#: 105106
Anti-mouse FcεRIα, Clone: MAR-1	BioLegend	Cat#: 134327
Anti-mouse IL-4, Clone: 11B11	BD Biosciences	Cat#: 557728
Anti-mouse/human IL-5, Clone: TRFK5	BioLegend	Cat#: 504303
Anti-mouse IL-13, Clone: eBio13a	Invitrogen	Cat#: 25–7133-82
Anti-mouse IFN-γ, Clone: XMG1.2	BioLegend	Cat#: 505810
Anti-mouse I-A[b], Clone: AF6-120.1	BD Biosciences	Cat#: 553552
Anti-mouse I-A/I-E (MHC II), Clone: M5/114.15.2	Biolegend	Cat#:107631

Reagent/Material	Source	Identifier
Anti-mouse I-A/I-E (MHC II), Clone: M5/114.15.2	Biolegend	Cat#: 107635
Anti-mouse I-A/I-E (MHC II), Clone: M5/114.15.2	Biolegend	Cat#:107626
Anti-mouse Ly6G/Ly6C (Gr-1), Clone: RB6-8C5	BioLegend	Cat#: 108412
Anti-mouse Siglec-F, Clone: E50-2440	BD Biosciences	Cat#: 552126
Biotinylated anti-Tuj1	BD Biosciences	Cat#: BAM1195
Fixable Viability Dye eFluor 780	Invitrogen	Cat #: 65-0865-14
TruStain fcX anti-mouse CD16/32, Clone: 93	Biolegend	Cat #: 101320
Critical Commercial Assays:		
Substance P ELISA Kit	Cayman Chemical Company	Cat #: 583751
CGRP (rat) EIA Kit	Cayman Chemical Company	Cat #: 589001
BD Cytofix/Cytoperm	BD Biosciences	Cat#: 554714
RNeasy Plus Micro Kit (50)	Qiagen	Cat #: 74034
RNeasy Plus Mini Kit (50)	Qiagen	Cat #: 74134
Experimental Models: Organisms and Strains:		
Mouse: C57Bl/6	Charles River Laboratory	Strain No.: 027
Mouse: C57Bl/6	The Jackson Laboratory	Strain No.: 000664
Mouse: B6(FVB)-Mgl2$^{tm1.1(HBEGF/EGFP)Aiwsk}$/J (CD301b-DTR)	The Jackson Laboratory	Strain No.: 023822
Mouse: Kaede^{+}	Tomura et al., 2008	
Mouse: NCI Br-Ly5.1/Cr	Charles River Laboratory	Strain No.: 564
Mouse: *Mrgpra1*$^{-/-}$	Meixiong et al., 2019	
Mouse: *Nav1.8*^{cre}	Abrahamsen et al., 2008	
Mouse: *Trpv1*^{DTR}	Pogorzala et al., 2013	
Mouse: *tdTomato*^{loxSTOPlox} [Ai14]	The Jackson Laboratory	Strain No.: 007908
Mouse: B6.Cg-*Kit*$^{W\text{-}sh}$/HNihrJaeBsmJ (Kit$^{w\text{-}sh/w\text{-}sh}$)	The Jackson Laboratory	Strain No.: 030764
Mouse: B6.Cg-*Tac1*^{tm1Bbm}/J (*Tac1*$^{-/-}$)	The Jackson Laboratory	Strain No.:004103
Mouse: 4get	Mohrs et al., 2001.	
Oligionucleotides for qPCR		
mMrgpra1 FWD (5’-GCAAGAGGAATGGGGGAAAGC −3’)	This manuscript	N/A
mMrgpra1 REV (5’-CCCGACCAGTCCGAAGATGAT −3’)	This manuscript	N/A
mMrgprb2 FWD (5’-ATCAAGAATCTAAGCACCTCAGC −3’)	This manuscript	N/A
mMrgpgrb2 REV (5’-GAAAGCAAAATCATGGCTTGGT −3’)	This manuscript	N/A
mTacr1 FWD (5’-CTTCACCTACGCAGTCCACAA,- 3’)	This manuscript	N/A
mTacr1 REV (5’-GGCTGAAGAGGGTGGATGATG −3’)	This manuscript	N/A
mTacr2 FWD (5’-GCTGACAGGTACATGGCCATTG −3’)	This manuscript	N/A
mTacr2 REV (5’TGGAGTAGAAACATTGTGGGGAGG −3’)	This manuscript	N/A
mTrpv1 FWD (5’-CCACTGGTGTTGAGACGCC −3’)	This manuscript	N/A
mTrpv1 REV (5’TCTGGGTCTTTGAACTCGCTG-3’)	This manuscript	N/A
Chemicals, Peptides, & Recombinant Proteins:		
TRIzol Reagent	Invitrogen	Ref #: 15596018

Reagent/Material	Source	Identifier
TritonX-100	Sigma-Aldrich	Cat#: T9284
Collagenase A	Sigma Aldrich	Cat#: 10103578001
Collagenase P	Sigma-Aldrich	Cat #: 11213857001
Dispase II	Sigma-Aldrich	Cat #: D4693–1G
DNase I, grade II	Sigma-Aldrich	Cat #: 10104159001
Dnase I Type IV	Sigma-Aldrich	Cat#: D5025
Liberase ™	Sigma-Aldrich	Cat #: 05401119001
Cytosine beta-D-arabinofuranoside	Sigma-Aldrich	Cat#: C6645
B-27 Supplement (50X)	Thermo Fisher Scientific	Cat#: 10889038
GlutaMAX	Gibco	Cat#: 35050061
Laminin	Sigma-Aldrich	Cat#: L2020
GDNF	Sigma-Aldrich	Cat#: G1401
Nerve Growth Factor 2.5S	Invitrogen	Cat#: 13257019
Papain	Sigma-Aldrich	Cat: 5125
Ovalbumin	Sigma-Aldrich	Cat: A5503
LPS	Invivogen	Cat: tlrl-eklps
Capsaicin	Sigma-Aldrich	Cat#: M2028
Histamine	Sigma-Aldrich	Cat#: H7125
Phospholipase A_2	Sigma-Aldrich	Cat #: P9279
Alternaria alternata	Greer Laboratories Inc	Cat#: NC1620293
Mite, House dust	Greer Laboratories Inc	Cat#: NC9756554
Calcitonin Gene Related Peptide (CGRP) powder	Sigma-Aldrich	Cat#:C0292–1MG
Substance P	Tocris	Cat#: 1156
QX314 chloride	Tocris	Cat#: 2313
QWF	Tocris	Cat#: 6642
L733,060 hydrochloride	Tocris	Cat#: 1145
Chloroquine diphosphate	Sigma-Aldrich	Cat#: C6628
Potassium chloride solution, 3M	Sigma-Aldrich	Cat#: 60137
Nle-Arg-Phe amide (FMRF)	Sigma Aldrich	Cat#: N3637
Normal Goat serum (NGS)	Jackson Immunoresearch	Cat#: 005–000-121
DMEM		
Krebs-Ringer Bicarbonate Buffer	Boston Bioproducts	Cat#: BSS-250
PBS	Corning	Ref #: 21–031-CV
Fura-2, AM	Thermo Fisher Scientific	Cat #: F1201
RBC Lysis buffer	Sigma-Aldrich	Cat #: R7757
0.5 M EDTA, pH 8.0	Gibco	Cat #: 15575–038
OCT Compound	Tissue-Tek	Cat #: 4583
DMEM	Corning	10–014-CV
RPMI 1640, 1X	Corning	Ref #: 15–040-CV

Reagent/Material	Source	Identifier
Neurobasal-A Medium	Thermo Fisher Scientific	Cat #: 10888
Fetal Calf Serum (FCS)	Atlanta Biologicals	Cat #: S11550
MultiScribe Reverse Transcriptase	Thermo Fisher Scientific	Ref #: 4311235
GeneAMP dNTP mix with dTTP	Thermo Fisher Scientific	Ref #: N8080260
$MgCl_2$ Solution 25 mM	Thermo Fisher Scientific	Ref #: 4486224
10x PCR Buffer II	Thermo Fisher Scientific	Ref #: 4486220
Oligio d(T)16	Thermo Fisher Scientific	Ref #: 100023441
Random Hexamers 50 μM	Thermo Fisher Scientific	Ref #: 100026484
RNase Inhibitor	Thermo Fisher Scientific	Ref #: 100021540
FastStart Essential DNA Green Master	Roche	Cat #: 25595200
Software:		
Prism v 7.0c	GraphPad	https://www.graphpad.com/demos
Zen Blue	Zeiss	https://www.zeiss.com/microscopy/us/products/microscope-software/zen.html
Imaris	Bitplane	http://www.bitplane.com/download
Softmax Pro	Molecular Devices	https://www.moleculardevices.com/systems/microplate-readers/softmax-pro-7-software
BD FACS Diva 8	BD Biosciences	http://www.bdbiosciences.com/us/instruments/clinical/software/flow-cytometry-acquisition/bd-facsdiva-software/m/333333/overview
FlowJo (version 10)	Tree Star	https://www.flowjo.com/solutions/flowjo/downloads